CHAPTER 5
A DYNAMIC MODEL OF THE ENTIRE ILMENITE-SMELTING FURNACE PROCESS

This chapter describes a dynamic model of the entire process contained in an ilmenite-smelting furnace. The model was used to conduct experiments to determine, under various circumstances, the influence of the slag bath on the freeze lining and crust, and the reverse influence of the freeze lining and crust on the slag bath. Details of these experiments are provided in CHAPTER 8 and CHAPTER 9.

5.1 IDENTIFICATION

The model being described in this chapter is identified as follows:

Name: Ilmenite-smelting Furnace Process Model

Abbreviation: ISFP model

5.2 PROBLEM DEFINITION

The main focus of this study was to investigate the dynamic interaction between the freeze lining and slag bath in an ilmenite-smelting furnace. All the influences to be considered have their origin in the slag bath, or first reach the slag bath before reaching the freeze lining. The slag bath therefore acts as a very important boundary condition to the freeze lining and crust models described in the previous two chapters. Because of the significance of the slag bath in this study, it was necessary to model, to a reasonable degree of accuracy, this part of the process for the use of the freeze lining and crust models to become more meaningful. Once the freeze lining and crust models had been integrated with a model that describes the slag bath well, this integrated model could be used as an improved representation of the dynamic behaviour of the slag bath, the freeze lining, the crust and of the process as a whole.

Since reduction reactions in the smelting process produce slag, metal and gas, modelling of the slag bath in isolation was not a meaningful option. For this reason the ISFP model described in this chapter had to be a comprehensive model of the ilmenite-smelting process. It had to take as inputs the material and energy inputs of the actual process (ilmenite, reductant, electrical energy). It also had to calculate as its final outputs the outputs of the actual process (liquid slag, liquid metal, off-gas and heat losses). Finally, intermediate states had to be calculated. These included the state of the slag bath, metal bath and furnace atmosphere.

In addition to the above, the model also had to integrate the freeze lining and crust models described earlier. This would enable it to also provide state information about the freeze lining and crust. These sub-models, especially the freeze lining sub-model, were the focus of most of the experiments described in subsequent chapters.

Because the focus of this study was more on the freeze lining and slag bath than on the rest of the process, the ISFP model was not required to provide the ultimate in accuracy in terms of modelling the metal bath, furnace atmosphere, etc. These aspects were modelled to such a degree of accuracy that satisfied the objectives of the study.

5.3 SYSTEM DESCRIPTION

Figure 8 (page 13) shows the aspects addressed by the ISFP model. A scale drawing was also made to present the furnace as it is described by the ISFP model (Figure 52 below). In this drawing the metal and slag baths are shown, as well as the areas (freeze lining and crust) described by the two conductor models presented in CHAPTER 3 and CHAPTER 4. The freeze lining as described by the FLC model is shown as being in contact with the sidewalls and slag bath. The crust described by the SBCC model is shown at the top part of the slag bath.

Material inputs enter the furnace through a hollow electrode. These materials include ilmenite and a reductant (typically anthracite or char). Material exits from the furnace as off-gas through an off-gas duct installed in the furnace roof, as slag through a slag tap hole and as metal through a metal tap hole. The metal tap hole is situated on a level lower than the slag tap hole because the metal has a higher density than the slag and it settles at the bottom of the furnace as a metal bath. Heat exits the furnace together with the material outputs just listed, and as heat lost through the furnace roof, sidewalls and hearth.

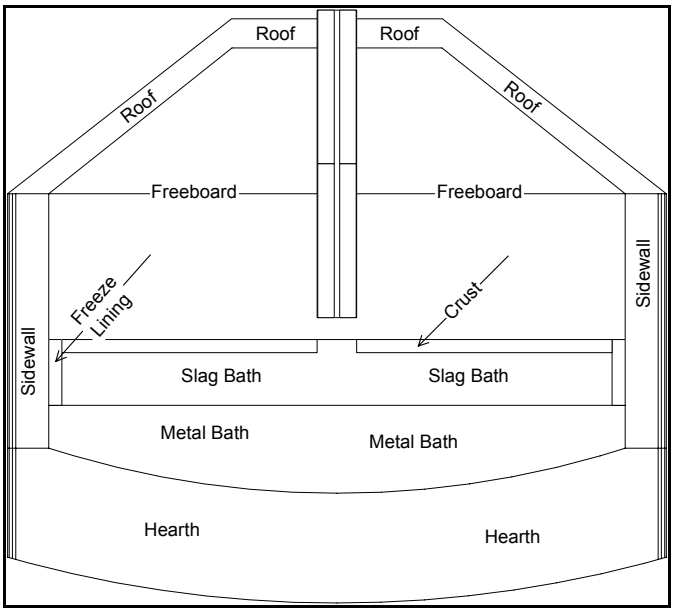

Figure 52 – Schematic of the furnace and process as described by the ISFP model.

The main areas of chemical reaction include the top of the slag bath where floating reductant particles react with liquid slag, the interface between the slag and metal baths where dissolved carbon in the metal reacts with liquid slag, and the turbulent region underneath the electrode where the arc attaches to the bath and material discharges into the bath. In all these zones the reaction products include slag, metal and gas.

5.3.1 Dimensions

The dimensions of the hypothetical system under consideration are presented in Figure 53 below.

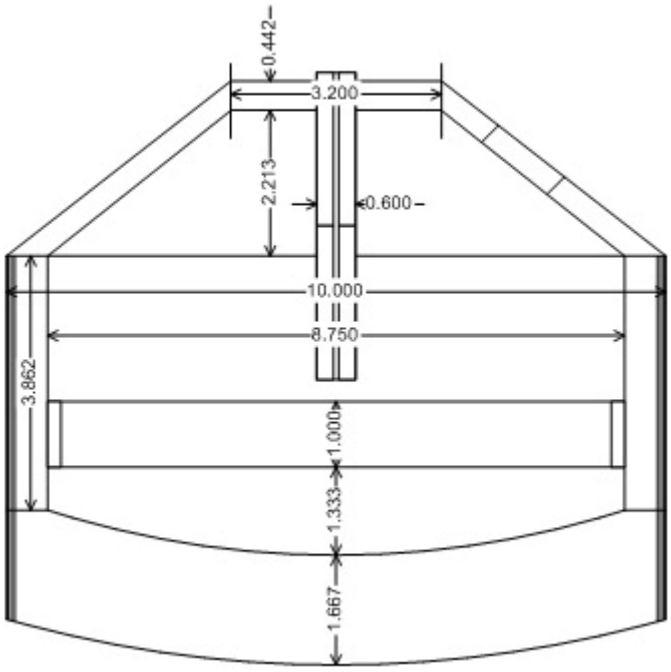

Figure 53 – Dimensions in meters of the furnace configuration used in CHAPTER 5.

5.4 KEY PHENOMENA

5.4.1 Heat Transfer

Figure 54 identifies the various heat transfer phenomena discussed in this section. The phenomena are referenced using the Q symbols presented in the schematic.

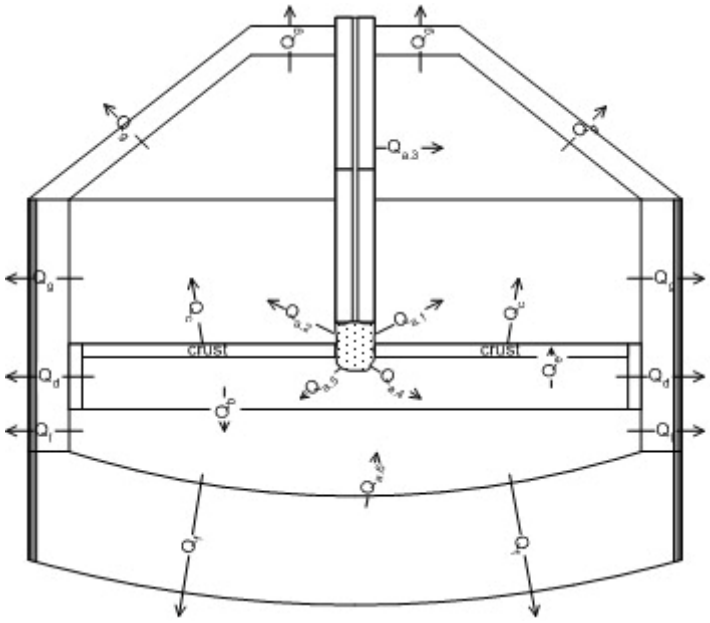

Figure 54 – Heat transfer phenomena in an ilmenite-smelting furnace.

a. Heat transfer from the arc

Because of the ilmenite-smelting furnace being powered by an electric arc, the arc is the main source of energy in the process. The electrical energy discharged into the furnace is distributed, in summary, between the furnace (walls, roof and freeboard) and the melt (slag and metal baths) (Stenkvist and Bowman, 1987). For an arc of 10 kA and 125 V, the distribution has been set out as follows (Stenkvist and Bowman, 1987):

- 28% to furnace
  - 20% via radiation ($Q_{a.1}$ in Figure 54)
  - 4% via convection ($Q_{a.2}$ in Figure 54)
  - 4% via the electrode effect ($Q_{a.3}$ in Figure 54)
- 72% to melt
  - 10% via radiation ($Q_{a.4}$ in Figure 54)
  - 50% via convection ($Q_{a.5}$ in Figure 54)
  - 12% via the electrode effect ($Q_{a.6}$ in Figure 54)

The electrode effect mentioned above refers to energy dissipated by resistance heating in either the graphite electrode (cathode) or in the slag bath, metal bath and bottom connection (anode).

The distribution presented above is specifically representative of a 10 kA and 125 V arc (power of 1.25 MW and resistance of 12.5 mΩ). Arcs with other current and voltage settings will result in different energy distributions. A higher arc resistance results in a longer arc and more radiation to walls, roof and freeboard, and less convection to the melt. However, the trend visible in the above distribution (that most of the energy is discharged into the melt via convection) should be present in general during the operation of actual furnaces.

Heat transfer from the arc was seen as a key phenomenon within the context of the ISFP model because of the arc being the main energy source of the process. However, the exact distribution of energy from the arc to the process was not viewed as being of major importance. For this reason it was decided to model the arc simply as an energy source into the bath. Details of the relative influences of radiation, convection and electrode effects were therefore ignored.

b. Heat transfer between slag bath and metal bath

Temperature gradients exist in the furnace from the high-temperature zone of the arc towards the outside boundaries of the furnace where the temperature is close to ambient. For this reason it has been observed that the metal bath (being further away from the arc) has a somewhat lower temperature than the slag bath. Energy flows from the slag bath into the metal bath, from which it flows into part of the freeze lining, sidewalls and hearth.

The mode of heat transfer from the slag bath to the metal bath is expected to be a combination of conduction and convection (Q_b in Figure 54). In the turbulent region below the electrode, convection is expected to be the dominant mechanism due to the intense movement and mixing in this region. In areas further away from the centre of the furnace convection is still expected to be dominant due to mixing that

is known to occur in these areas in both the slag and metal baths. Conduction should however play a relatively larger role compared with the zone under the electrode.

Heat transfer between the slag and metal baths was not viewed as critical to the ISFP model. It was decided to assume that the slag and metal baths existed at the same temperature (Assumption 5.1, page 110).

c. Heat transfer from the slag bath surface to the furnace freeboard

Extensive modelling work was done on radiation in the freeboards of DC smelting furnaces (Reynolds, 2002). That study showed that radiation from the bath surface is the main source of energy loss into the freeboard and through the upper sidewalls and roof.

The impact of heat losses from the slag bath surface was seen as important to the ISFP model. The detailed mechanisms of heat transfer in this region were however not viewed as being that important. For this reason it was decided to describe heat transferred from the slag bath surface by a simple heat transfer coefficient boundary condition derived from the work by Reynolds (2002).

d. Heat transfer from the slag bath to the freeze lining and sidewall

Heat transfer from the slag bath to the freeze lining and sidewall was of critical importance to the ISFP model because the model was required to describe interactions between the slag bath and the freeze lining. For details about the heat transfer phenomenon, refer to CHAPTER 3.

e. Heat transfer from the slag bath to the crust

Because the ISFP model was also required to model interactions between the crust and the slag bath (in cases when a crust exists), this heat transfer phenomenon was viewed as being important. Details about this heat transfer component are included in CHAPTER 4.

f. Heat transfer from the metal bath to the sidewalls and hearth

A significant amount of energy is lost from the metal bath to the lower sidewalls and hearth. The heat is transferred through convection to these surfaces, and by conduction through the sidewalls and hearth towards the outside of the furnace. Heat is removed by water cooling in the case of the sidewalls and either water or air cooling in the case of the hearth.

This phenomenon was seen as important to the ISFP model. It was however decided to incorporate it into the model as two simple boundary conditions, and not as comprehensive models describing convection and conduction heat transfer.

g. Heat transfer through the upper sidewalls and roof

Heat transferred into the freeboard from the arc and slag bath surface by convection and radiation reaches the upper sidewalls and roof. This heat is transferred toward the outside of the furnace through conduction. The upper sidewalls, the conical part of the roof and the flat part of the roof are all covered with a layer of process material (Reynolds, 2002). In an ilmenite-smelting furnace, this layer consists of slag, ilmenite and reductant particles.

In the case of the upper sidewalls (the walls above the level of the slag bath surface), the heat that arrives at the hot face from the furnace freeboard is removed by conduction through the layer of process material, the brick layer, potentially a ramming layer and the steel shell. Forced water cooling is often applied on the outside of the shell.

The conical part of the roof often does not contain a brick layer. Heat from the freeboard is therefore removed by conduction through the layer of process material and steel shell, and by forced water cooling on the outside of the steel shell.

The flat part of the roof again has a layer of refractory material. Conduction is therefore responsible for removing heat from the freeboard. On the outer surface of the flat part of the roof no forced cooling is used.

The heat removed from the system by the above-mentioned mechanisms was seen as important to the ISFP model, but the detailed mechanisms were not viewed as being important enough to include in the model. As mentioned in paragraph c above, an effective heat transfer coefficient from the top of the slag bath surface was used to model all heat transferred upward from the slag bath surface.

5.4.2 Mass Transfer

When describing mass transfer below, the phenomena were classified as follows:

- Bulk flow.

  Bulk flow refers to phenomena such as ore and reductant that are fed into the furnace through the hollow electrode, or metal and slag that are tapped from the furnace through the tap holes.

- Convective mass transfer.

  This refers to mass flow resulting from fluid flow within a single phase. For example, carbon dissolved in iron is transported to the surface between the slag and metal baths as a result of stirring in the metal bath.

- Diffusion

  Diffusion refers to mass transfer resulting from concentration gradients in a phase. For example, Ti_2O_3 diffuses away from the interfaces at which reduction takes place into the bulk slag phase due to reduction increasing the Ti_2O_3 concentration at the reaction interface.

In the drawings describing the various mass flow phenomena below, the symbol m_B is used to indicate bulk mass flow.

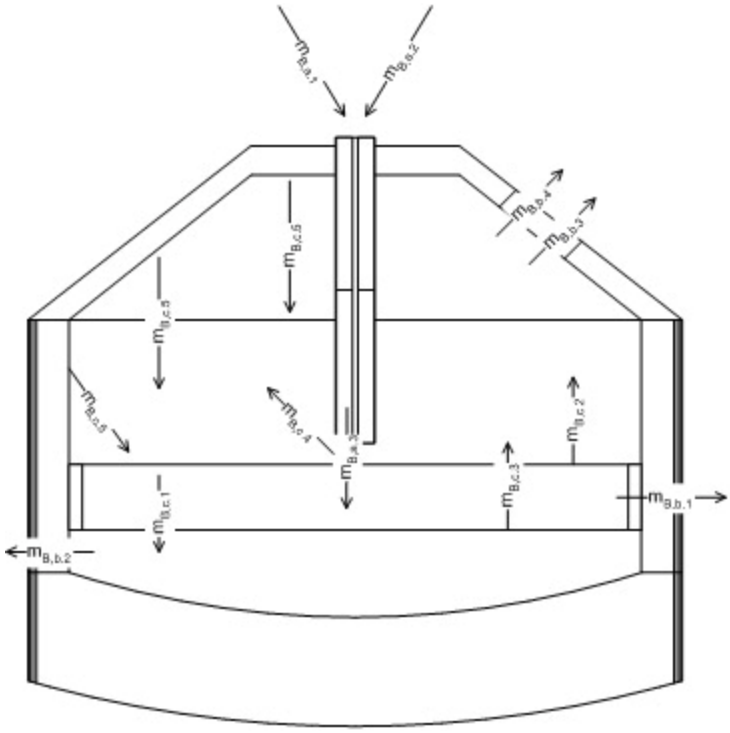

Figure 55 – Bulk mass flow phenomena in an ilmenite-smelting furnace.

a. Bulk mass flow of feed materials

The main feed materials, ilmenite ($m_{B,a.1}$) and reductant ($m_{B,a.2}$), are fed into the furnace through the hollow graphite electrode. The material accelerates under the influence of gravity and enters the slag bath with significant momentum. This momentum adds to the turbulence in the zone below the electrode.

The graphite electrode is consumed at its tip. Graphite released into the process in this way also represents a bulk mass flow stream ($m_{B,a.3}$). This graphite is expected to enter into the slag bath and freeboard as a result of the flow of the arc plasma.

Because ilmenite and the carbon-based reductant are the main feed components of the process, the bulk flows of these materials were very important within the context of the ISFP model. Both these flows were therefore incorporated in the model. The flow of graphite (from the electrode material), however, was not seen as equally important. This flow was ignored, but it can be viewed that the graphite flow was incorporated in the reductant bulk flow.

b. Bulk mass flow of product materials

The main products of the process are slag tapped from the slag bath ($m_{B,b.1}$) and metal tapped from the metal bath ($m_{B,b.2}$). The third stream exiting the furnace contains gas (mainly CO; $m_{B,b.3}$), fume and dust ($m_{B,b.4}$).

Three of these four bulk mass flow streams had to be incorporated into the model. This is because slag, metal and gas are inevitably produced inside the furnace when feed materials and energy are charged. It

was however decided that the dust bulk flow stream ($m_{B,b.4}$) was of lesser importance to the ISFP model, and it was therefore ignored.

c. Internal bulk mass flow phenomena

The reduction reactions taking place between slag and reductant particles in and on top of the slag bath produce metal droplets as one of its products. Such droplets continuously travel down through the slag bath and coalesce with the metal bath ($m_{B,c.1}$).

This bulk flow was incorporated into the ISFP model in a crude way by moving all metal produced by reduction reactions immediately to the metal bath once it was produced.

Another product of the same reduction reactions is gas. Gas travels up through the slag bath and into the freeboard as it is produced ($m_{B,c.2}$).

Reduction reactions also occur at the interface between the slag and metal baths due to the relatively high carbon content of the metal bath (around 2%). These reactions also produce gas that travels up through the slag bath and into the freeboard ($m_{B,c.3}$).

The two gas bulk flows described above were handled similar to the metal bulk flow by moving all gas produced by reduction reactions immediately to the freeboard.

Due to the significant momentum transferred to the slag bath by the entering feed material and arc, material is thrown from the zone underneath the arc into the freeboard and towards the sidewalls and roof ($m_{B,c.4}$). Since these furnaces do not continue to build up material on the sidewalls and roof and eventually clog up completely, it can be safely assumed that some material also travels back from the sidewalls and roof into the slag bath ($m_{B,c.5}$). This is likely due to melting of such material by heat radiated to these surfaces.

The bulk flow of material to and from the upper sidewalls and roof was not seen as important to the ISFP model. These flows were therefore ignored.

d. Mass transfer at the slag–reductant interface

The most important reaction interface in the process is believed to be the interface between liquid slag and reductant particles. Reactions at this interface result in the formation of metal, gas and a slag enriched in Ti_2O_3.

It is expected that diffusion will occur in the slag phase due to the Ti_2O_3 concentration gradient created by reduction reactions. Due to stirring in the slag bath, it is also expected that liquid slag and reductant particles will move relative to each other. In the case of the slag phase, this can be viewed as convective mass transfer to and from the slag–reductant interface. This causes a renewal of liquid slag taking part in reduction reactions at this interface.

Metal and gas formed during reduction reactions are carried away from the slag–reductant interface by buoyancy forces due to the marked difference in density between these materials and liquid slag. These phenomena were classified as bulk mass flows in paragraph c above.

The diffusion and convective mass transfer phenomena identified above were viewed as important to the ISFP model. However, it was decided not to model these phenomena in any great detail, but rather to incorporate it into the model by a simple approach (paragraph 5.6.8a, page 125).

e. Mass transfer at the interface between the slag and metal baths

Reduction reactions also take place at the interface between the slag and metal baths. The reason for these reactions is the relatively high carbon content of the metal (around 2%) that is not in equilibrium with the liquid slag. Carbon therefore reacts with FeO and TiO_2 in the slag to form CO gas, Fe metal and Ti_2O_3. The metal product of the reduction reaction is expected to coalesce with the metal bath virtually immediately. The CO gas bubbles move upward through the slag bath to eventually escape into the freeboard (paragraph c above).

The slag at the interface becomes depleted in FeO and TiO_2, and enriched in Ti_2O_3. This causes concentration gradients in the slag phase that will result in diffusion of these species. Ti_2O_3 will tend to diffuse away from the interface and FeO and TiO_2 are expected to diffuse toward the interface.

In the case of the metal phase carbon is consumed at the interface. The metal will therefore become depleted in carbon. The resulting carbon concentration gradient will cause carbon to diffuse toward the interface from the bulk metal.

Significant stirring is known to occur in both the slag and metal baths. This stirring causes convective mass transfer on both sides of the interface. This convective mass transfer results in the renewal of both slag and metal at the interface from the respective bulk phases. It is expected that convective mass transfer is the dominant mass transfer mechanism at this interface.

The mass transfer phenomena identified above were viewed as important to the ISFP model. The detailed modelling of these phenomena was however excluded to simplify the model. The phenomena were incorporated into the model by a simple approach (paragraph 5.6.8b, page 129).

f. Mass transfer of carbon into the metal bath

One phenomenon in the ilmenite-smelting process that is not yet understood clearly is the transfer of carbon into the metal bath. As mentioned above, the metal carbon content of around 2% observed in ilmenite-smelting processes (Geldenhuis and Pistorius, 1999) is far from the composition for metal in equilibrium with slag (which is less than 0.2% according to simple FactSage equilibrium calculations). This causes reduction reactions to take place at the interface between the slag and metal baths. These reactions contribute to lowering the carbon concentration of the metal bath. This creates a question: What causes the carbon content of the metal to increase to a value of around 2% if reduction reactions at the interface between the slag and metal bath tend to lower the composition toward 0.2% carbon?

At least two possible phenomena exist that can contribute to increasing the carbon content of the metal. Firstly, it is possible that the turbulent zone underneath the electrode may consist of a mixture of slag, reductant particles and metal droplets. Assuming that this is true, the metal droplets in the region can come into contact with reductant particles under conditions of high temperature. It is not certain what the typical

temperature in this region is, but with slag being tapped at temperatures in excess of 1700°C, it is likely that the temperature of the zone underneath the electrode could be substantially higher.

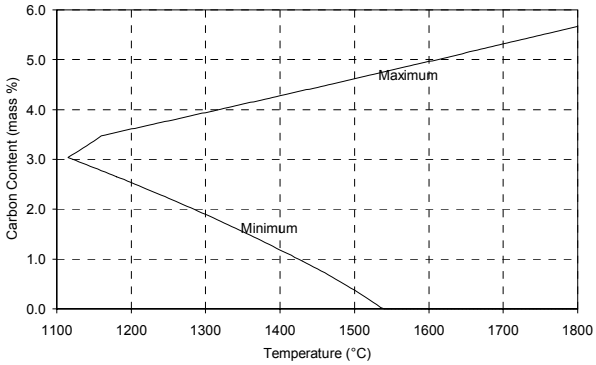

Figure 56 – Solubility limits of carbon in liquid iron as functions of temperature. (FactSage 5.2)

Figure 56 shows the solubility limits of carbon in liquid iron. The maximum solubility indicates the maximum carbon content of liquid iron at a specific temperature. The minimum limit indicates the minimum carbon content of liquid iron at a specific temperature. Both these limits are indicated for equilibrium conditions. Other solute elements such as Ti, Mn, S, etc. were not taken into account. From this figure it is clear that the maximum solubility of carbon increases with increasing temperature. At a temperature of 1800°C liquid iron can contain up to 5.67 % carbon (by mass).

If the turbulent zone under the electrode is at a temperature of 1800°C and liquid metal droplets come into contact with reductant particles, these droplets can be carburised up to a carbon content of around 5.67 % before reaching carbon saturation. It is however expected that droplets will not have long residence times in the turbulent zone before being reabsorbed into the metal bath. It is therefore not certain whether these droplets will reach the point of carbon saturation. Nevertheless, it is likely that these droplets will be carburised to some extent in this zone, thereby contributing to an increase in metal bath carbon content.

The second phenomenon that may increase the carbon content of the metal bath also involves small metal droplets, but in this case the droplets originating from reduction reactions at the slag–reductant interface. These droplets may leave the reduction reaction zone with high carbon contents as a result of contact with reductant particles present. Once again Figure 56 indicates that up to 5.31% carbon (by mass) can be dissolved in liquid iron at a temperature of 1700 °C that can be attained in this area.

The droplets produced at the slag–reductant interface still have to travel down through the slag bath and into the metal bath. During this journey the droplets are likely to be in contact with liquid slag, but less likely to remain in contact with reductant particles. Because it was already calculated that metal with high carbon content will tend to react with slag, these droplets will tend to lose most of their carbon while travelling to the metal bath.

The phenomenon of carbon mass transfer into the metal bath was seen as important to the ISFP model because realistic metal bath carbon contents were required to make reduction reactions possible at the

interface between the slag and metal baths. For this reason both of the phenomena described above had to be incorporated into the model. The second phenomenon could be implicitly incorporated in the reduction reactions between slag and reductant particles. The carbon content of metal produced from these reactions could simply be a function of the thermodynamic equilibrium behaviour of this part of the process. The first phenomenon where reductant particles come into contact with metal droplets in the turbulent zone underneath the electrode had to be incorporated explicitly into the model by a reaction interface between metal and reductant.

g. Mass transfer at the interface between the slag bath and freeze lining

As observed from the experimental results in CHAPTER 6, solidification and melting at the interface between the slag bath and freeze lining cause changes in liquid slag composition at this interface. In the case of solidification the FeO and TiO_2 contents increase and the Ti_2O_3 content decreases. During melting of the freeze lining the opposite was observed.

These changes in liquid slag composition at the interface cause diffusion in the liquid slag. More importantly, the convective mass transfer resulting from strong mixing in the slag bath transports liquid slag to and from this interface.

These phenomena were addressed in CHAPTER 3 as part of the FLC model and were treated in the same way in the ISFP model.

5.4.3 Momentum Transfer

a. Momentum sources

There are five main sources of momentum in the process:

- The plasma arc.
- Feed material falling into the bath.
- Electromagnetic stirring.
- Gas rising up through the metal bath and into the freeboard.
- Buoyancy forces in the slag and metal baths.

The momentum sources discussed below were viewed to be important collectively to the ISFP model. However, details of flow phenomena associated with these sources were not viewed as important. It was decided to incorporate the influence of these momentum sources into the ISFP model by assuming that the slag and metal baths both are ideally mixed (Assumption 5.2, page 110; Assumption 5.3, page 111).

i. The plasma arc

The plasma arc on its own and in combination with feed material transfers a significant amount of momentum to the bath. No quantitative information was available for inclusion here, but some qualitative and some related quantitative information should give the reader an indication of the amount of momentum involved.

It was reported by Stenkvist and Bowman (1987) that a 40 kA arc operating with a gap of 300 mm between the cathode tip and the bath surface creates a 160 mm depression in a bath of molten iron metal. The same authors reported that the maximum axial velocity associated with an arc current of a mere 200 A was measured to be approximately 330 m/s.

Ramírez-Argáez (2003) reported that shear stresses of the arc on the bath surface, when viewed in isolation, can cause velocities of around 0.5 m/s in a metal bath (depth 0.5 m and diameter 3 m). Shear stresses, however, are never the only influence causing movement in the bath. It is always combined with effects of buoyancy and electromagnetic stirring.

From the above it can be concluded that the plasma arc acts as a major momentum source in the process.

ii. Feed material

In the case of the scale drawing shown in Figure 52, material entering the furnace would fall a minimum of around 5 m through the hollow electrode column. The roof configuration in this drawing is probably higher than for furnaces found in practice. It is expected that the minimum distance material would fall in practice would be around 3 m. Assuming unconstrained movement of feed material in the hollow electrode, the velocity of the feed material after a fall of 3 m is approximately 7.75 m/s (27.9 km/h). This relates to momentum of 71 kg.m/s being added to the bath per second when feeding 30 ton of ilmenite and 3 ton of reductant per hour (a total of 33 ton/h or 9.2 kg/s). The actual momentum is expected to be less than this due to movement of feed material in the hollow electrode being constrained to some degree.

The momentum carried into the furnace with the feed material is expected to cause significant motion in at least the zone underneath the electrode. This momentum together with the momentum of the arc is responsible for the turbulence in this zone.

iii. Electromagnetic stirring

Ramírez-Argáez (2003) reported that electromagnetic forces are dominant in establishing velocity gradients in a metal bath. The motion caused by electromagnetic stirring was shown to be opposed by the motion caused by shear stresses from the arc and buoyancy forces. The combination of these influences resulted in a maximum velocity of 1.22 m/s in a metal bath without a slag covering. When a slag layer was introduced, the maximum velocity in the system dropped to 0.4 m/s. The system modelled by Ramírez-Argáez (2003) had a metal bath depth of 0.5 m and a diameter of 3 m.

iv. Rising gas

Gas bubbles produced by reduction reactions at the interface between the slag and metal baths, and at interfaces between slag and reductant particles dispersed throughout the slag bath rise up through the slag bath and escape into the freeboard. The creation and movement of this gas is expected to transfer some momentum to the surrounding liquid slag, thereby influencing fluid flow in the slag bath.

v. Buoyancy forces

Temperature gradients in the slag and metal baths cause variations in density of these materials. This causes lower-density material to travel upward, and higher-density material to travel downward under the

influence of buoyancy forces. The influence of buoyancy was studied by Ramírez-Argáez (2003), and it was found to have a lesser influence on flow in a metal bath compared to shear forces from the arc and electromagnetic influences.

b. Momentum transfer in the slag bath

All five sources of momentum listed and described above are expected to influence fluid flow in the slag bath. The most pronounced influence is expected to result from momentum transferred from the arc and feed material entering the bath in the centre underneath the electrode. The impinging stream of plasma and feed material is believed to be so intense that it will cause some material to be projected toward the sidewalls of the furnace. This effect can be compared with blowing air through a straw onto the surface of a glass of water. When one blows hard enough some water droplets are projected toward the sides of the glass.

Due to the relatively high electrical conductivity of high-titania slag (Pistorius and Coetzee, 2003) it is expected that electromagnetic forces will have some influence on fluid flow in the bath. The exact magnitude of these influences is however not known.

Because gas is produced by reduction reactions at the interface between the slag and metal baths, gas will rise up through the slag bath. This gas is expected to influence fluid flow in the slag bath to some degree. Since most reduction reactions are expected to occur at the interface between reductant particles and liquid slag, and not at the interface between the metal and slag baths, the flow of gas rising through the slag bath from the top of the metal bath is expected to be low. For this reason the contribution to fluid flow in the slag bath from gas bubbles rising up through the slag bath is expected to be small relative to the influences of feed material, the arc and electromagnetic stirring.

Some vertical temperature gradients are expected in the slag bath due to the heat sink caused by reduction reactions occurring between reductant particles and liquid slag on the slag bath surface. Such temperature gradients are expected to cause variations in density. The extent of the flow caused by the resulting buoyancy forces is unknown.

Details of flow phenomena occurring in the slag bath were ignored. The influence of these phenomena was incorporated into the ISFP model by assuming ideal mixing in the slag bath (Assumption 5.2, page 110).

c. Momentum transfer in the metal bath

Momentum from the arc and feed material is expected to influence the metal bath. The extent of this influence depends on feed rate, electrical parameters (power, current) and the depth of the slag bath. Because of the metal bath being somewhat separated from the arc and feed material by the slag bath, it is expected that these momentum sources will have a lesser influence on flow patterns in the metal bath.

Because of the metal bath being similar to the metal bath studied by Ramírez-Argáez (2003) in terms of composition, the relative influences of different phenomena on flow in the metal bath of an ilmenite-smelting furnace can be expected to be similar. For this reason it is expected that electromagnetic stirring will also be dominant in establishing flow patterns in the metal bath of an ilmenite-smelting furnace. It was reported (Ramírez-Argáez, 2003) that velocities in the metal bath can be around 0.4 m/s when a slag layer

is present. This was calculated for a metal bath with a depth of 0.5 m and a diameter of 3 m. It is unknown what the velocities in the metal bath would be for the geometry used in the current study.

Finally, buoyancy forces are expected to have only a slight influence on flow in the metal bath. The reason for this is that the direction of heat transfer in the bath is predominantly downward. Such heat transfer would cause thermal stratification of the metal bath with colder material collecting at the bottom of the furnace and hotter material remaining above. The metal bath is not stagnant, however. As already mentioned the arc, entering feed material and electromagnetic forces are all expected to cause flow in the metal bath. Such flow is likely to cause hot material to move toward the bottom of the furnace. In such a case buoyancy forces will tend to 'push' such material upward.

Again, details of flow phenomena in the metal bath were not seen as critically important for the ISFP model. All these phenomena were incorporated into the model using the assumption that the metal bath is ideally mixed (Assumption 5.3, page 111).

d. Momentum transfer in the freeboard

Flow in the freeboard of the furnace is expected to be influenced mostly by the following factors:

- The arc.
- Gas rising up from the slag bath.
- Buoyancy forces.

Figure 57 shows flow patterns in an empty (no feed) arc operating at 30 kA and 270 V. On this drawing it is clear that gas from the surroundings of the arc (the freeboard) is drawn into the arc at the top and middle of the arc column, and then ejected at the bottom of column. Because of the high velocities that have been measured for even small arcs (330 m/s for a 200 A arc (Stenkvist and Bowman, 1987)) the arc can be viewed as a 'pump' causing significant motion in the furnace freeboard.

Reduction reactions cause gas (approximately 150 kg per ton of ilmenite fed) to be released into the furnace freeboard. This relates to 3.75 t/h and approximately 21,600 m^3/h (or 1.04 kg/s and 6.01 m^3/s) of gas released into the freeboard when operating a furnace at 25 ton/h ilmenite. (Volumes were calculated at 1 atm pressure and 1700 °C.) Because this gas has to exit the furnace through a gas off-take installed in the furnace roof, the average flow of gas in the furnace freeboard has to be directed upwards and towards the off-take. Because this bulk flow rate of gas is relatively low, the flow velocities caused by it are expected to be small.

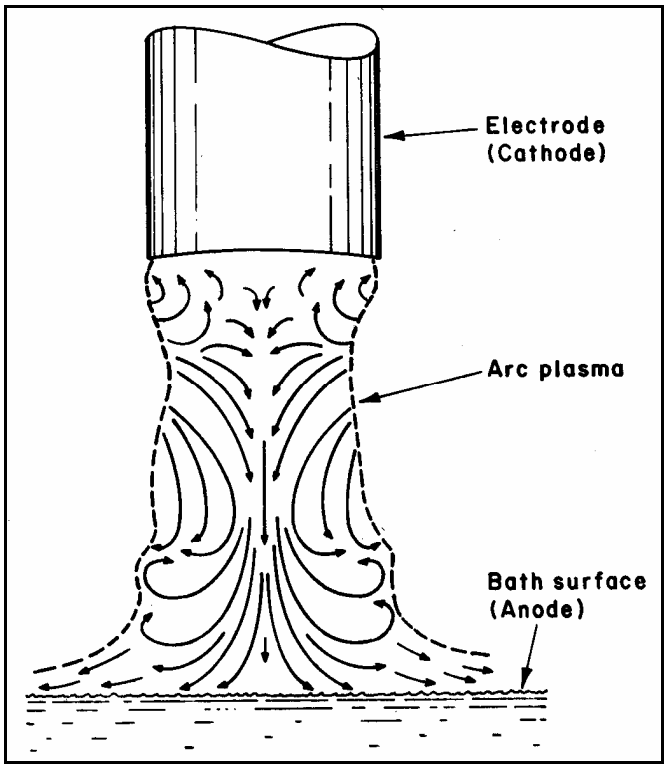

Figure 57 – Flow patterns in a 30 kA, 270 V arc. (Stenkvist and Bowman, 1987)

Gas enters the freeboard at approximately the temperature of the slag bath. Gas in the freeboard exchanges heat with the sidewalls and roof by convection and radiation. These exchanges are expected to cause variations in gas temperature (and therefore gas density) in the freeboard. These variations are then expected to result in buoyancy forces and flow in the freeboard.

Because gas has a relatively low contact and residence time in the system being considered, details of flow phenomena in the freeboard were viewed as unimportant to the ISFP model. For this reason the freeboard was assumed to be ideally mixed (Assumption 5.4, page 111).

5.4.4 Chemical Reaction

Chemical reactions take place at numerous locations in the furnace between and within various phases. This paragraph describes briefly most of the reactions occurring in the furnace and their importance to the ISFP model. The discussions are organised by focussing on specific phases or materials and grouping reactions that are of specific interest to that phase or material. The following list presents the phases and materials that are used to organise the discussions below:

- Liquid slag
- Solid slag
- Liquid metal
- Reduction product gas
- Air
- Graphite

a. Chemical reactions involving liquid slag

Since liquid slag is the primary product of the process, chemical reactions involving this phase are naturally very important. Of specific relevance to the liquid slag are its chemical reaction with ilmenite, reductant, refractory material and chemical reactions within the liquid slag phase.

i. Reaction between liquid slag and ilmenite

As feed material enters the furnace through the hollow electrode, through the arc and into the turbulent zone beneath the arc, at least some ilmenite particles are expected to melt. Due to the relatively short residence time of material flowing at high rates through small volume occupied by the arc some ilmenite particles are expected to arrive in the bath still in the solid state.

Due to the high temperature of the slag bath (1620 to 1680 °C [Geldenhuis and Pistorius, 1999]) and the even higher temperatures prevailing in the zone beneath the arc, ilmenite particles arriving in the bath in the solid state are expected to melt quickly. This is due to the relatively low melting point of ilmenite of around 1397 °C (FactSage 5.2).

Because of the reduction work that is continuously being done in the furnace, the liquid slag in the slag bath exists in a more reduced state compared with molten ilmenite. The newly-melted ilmenite will therefore tend to oxidise the liquid slag. The following reactions are expected to occur:

$$(Fe_2O_3)_{ilmenite} + (Ti_2O_3)_{slag} \rightarrow 2(FeO) + 2(TiO_2)$$

$$(FeO)_{ilmenite} + (Ti_2O_3)_{slag} \rightarrow (Fe^{\circ}) + 2(TiO_2)$$

The subscripts *ilmenite* and *slag* used above indicate the origin of the species within the context of the current discussion. Liquid ilmenite and slag do not exist as two separate phases. Further, the species indicated above exist in ionic form in the slag and the reactions will tend to be redox reactions between cations. This applies to all reactions described subsequently that involve liquid slag phase constituents.

The reactions described above were of critical importance to the ISFP model and was incorporated into the model.

ii. Reaction between liquid slag and reductant

Reduction of liquid slag by solid reductant particles is the primary means of converting feed material to products in the process. The following reactions are expected to occur:

$$(Fe_2O_3)_{slag} + (C)_{reductant} \rightarrow (FeO)_{slag} + (CO)_{gas}$$

$$(FeO)_{slag} + (C)_{reductant} \rightarrow (Fe^{\circ})_{metal} + (CO)_{gas}$$

$$2(TiO_2)_{slag} + (C)_{reductant} \rightarrow (Ti_2O_3)_{slag} + (CO)_{gas}$$

The reactions described above were of critical importance to the ISFP model and were incorporated into the model.

iii. Reaction between liquid slag and liquid slag

Reduction reactions occurring at the interface between liquid slag and reductant particles may occur to such an extent that the products of these reactions are more reduced than the bulk liquid slag. In such a case the reduction products would tend to reduce some species in the bulk liquid slag.

$$(Ti_2O_3)_{slag} + (FeO)_{slag} \rightarrow 2(TiO_2)_{slag} + (Fe^{\circ})_{slag}$$

The above reaction was of critical importance to the ISFP model and was incorporated into the model.

iv. Reaction between liquid slag and liquid metal

Reduction reactions occurring at the interface between the slag and metal baths occur because of the high carbon content of the liquid metal. The following reactions are expected to occur.

$$(FeO)_{slag} + (C)_{metal} \rightarrow (Fe)_{metal} + (CO)_{gas}$$

$$2(TiO_2)_{slag} + (C)_{metal} \rightarrow (Ti_2O_3)_{slag} + (CO)_{gas}$$

The above reactions were of critical importance to the ISFP model and were incorporated into the model.

v. Reaction between liquid slag and refractory material

As has been discussed in CHAPTER 2, no known refractory material can withstand the chemical attack of liquid high-titania slag. The high-MgO refractory brick used in ilmenite-smelting furnaces simply dissolves in liquid slag if it is not protected by a freeze lining.

Reactions involving refractory materials were not viewed as important to the current study and were therefore omitted from the ISFP model.

b. Chemical reactions involving solid slag

Chemical reactions involving solid slag have been discussed in CHAPTER 3 and CHAPTER 4. The reader is referred to paragraphs 3.4.4 (page 32) and 4.4.4 (page 68).

c. Chemical reactions involving liquid metal

i. Reaction between liquid metal and reductant

It is suspected that reductant particles come into contact with liquid metal in the turbulent zone underneath the electrode. This contact is expected to result in the dissolution of carbon and other species in liquid metal.

$$(C)_{reductant} \rightarrow (C)_{liquid\ metal}$$

The above reaction was viewed as important and was included in the ISFP model.

ii. Reaction between liquid metal and refractory material

According to equilibrium calculations with FactSage 5.2, some interaction between the liquid metal phase and MgO refractory brick can occur. The calculations indicated a very small amount of FeO (0.001%) being

taking up into a monoxide solid solution phase with MgO. Some Mg (0.004%) and MgO (0.002) were also observed in the calculated state of the liquid metal phase.

The above dissolution reactions were not viewed as being of significant importance to the ISFP model. For this reason they were omitted from the model.

d. Chemical reactions involving reduction product gas

i. Reaction between gas and liquid slag

Gas bubbles rising up through the liquid slag layer are expected to interact with the surrounding slag. Should this gas come into contact with slag that is more oxidised (higher P_{O2}) than the environment in which the gas was formed, the composition of the gas bubble would shift to containing more CO_2 and H_2O and less CO and H_2. If it comes into contact with slag that is more reduced than its initial composition, the composition of the gas in the bubble will shift in the opposite direction.

Reactions involving gas after reduction were seen as unimportant to the ISFP model. The reason for this is that the shifts in gas composition mentioned above proved to be very slight when studying it with FactSage 5.2. These reactions were therefore ignored. It was assumed that all gas formed as a result of reduction reactions immediately escapes into the freeboard and does not come into contact with slag, metal or reductant again (Assumption 5.5, page 111).

ii. Reaction between gas and reductant

It is expected that gas that formed as a result of reaction between liquid slag and solid reductant may remain in contact with the reductant particle that it originated from. This gas may act as an intermediate layer between liquid slag and solid reductant. The reactions taking place in this gaseous layer with liquid slag on one side and solid reductant on the other are expected to be as follows:

$$2(TiO_2)_{slag} + (CO)_{gas} \rightarrow (Ti_2O_3)_{slag} + (CO_2)_{gas}$$

$$(C)_{reductant} + (CO_2)_{gas} \rightarrow 2(CO)_{gas}$$

FactSage 5.2 was used to determine the limiting extents of the two reactions above. First pure CO was brought into contact with a 15-55-30 (FeO-TiO_2-Ti_2O_3 mass percentages) slag at 1700 °C. The result was that the gas phase reached a composition of 93.3-6.7 (CO-CO_2 volume percentages) and some TiO_2 was reduced to Ti_2O_3. Pure CO_2 was then brought into contact with pure graphite at the same temperature. The result was a gas containing virtually 100% CO.

These results show that pure CO gas has only limited capacity to reduce liquid high-titania slag at furnace operating temperatures. It was concluded that inclusion of a gas-reductant interface would not add significantly to the ability of the ISFP model to describe the process. These reactions were therefore excluded from the model and the assumption that all gas formed as a result of reduction reactions immediately escapes into the freeboard was applied again (Assumption 5.5, page 111).

e. Chemical reactions involving air

It is well known that some air is drawn into the furnace during operation due to fluctuations in furnace pressure. The oxygen entering the system in this way tends to increase the oxygen potential in the system slightly. This results in increased consumption of reductant. The entrained air is expected to react primarily with gas in the freeboard to combust CO and H_2 to CO_2 and H_2O. Since the freeboard gas is extracted via the gas off-take, the residence time of the combusted species in the furnace is expected to be small. The influence of entrained air on the process is therefore expected to be limited.

Reactions of air with gas during operation were seen as unimportant to the current work. For this reason these reactions were omitted from the ISFP model. It was assumed that no air enters the furnace during operation (Assumption 5.6, page 112).

Large volumes of air are drawn into the system when the furnace is shut down for maintenance and inspections. During such times the furnace pressure is controlled at a negative value relative to ambient. The air entering the furnace during such periods is expected to react with reductant on the slag bath surface, liquid slag at the slag bath surface and with the solid slag crust once such a crust has formed. The implications of these reactions are that oxygen is added to the process and carbon is removed. This exactly opposes the objectives of the process. The end result of such periods of down time is that additional energy and reductant have to be added to the process to bring it back to the desired operating state.

The influence of air on the process during periods of down time can certainly be significant. Phenomena associated with air exposure were however not the focus of the current work. For this reason all reactions related to air exposure during periods of down time were omitted from the ISFP model. It was assumed that no air enters the furnace during periods of down time (Assumption 5.7, page 112).

f. Chemical reactions involving graphite

The graphite electrode column is exposed to reaction with many phases in the process. It is expected that slag and, to a lesser extent, metal are splashed onto the lower part of the column. Slag is expected to be reduced by the graphite and some graphite is expected to dissolve into liquid metal droplets. In both these cases graphite is consumed on the surface of the column. This results in increased electrode consumption.

The largest part of the electrode column present inside the furnace is exposed to gases in the furnace freeboard. Since reduction product gas is highly reduced (low P_{O2}), this gas is not expected to have a major influence on the column.

Air drawn into the furnace during normal operation could adversely affect the electrode. Because it is likely that at least some of the air drawn in will enter the furnace between the electrode column and the seal surrounding it in the flat part of the furnace roof, it is also likely that some of this air will react with the hot electrode column at this location. This can increase electrode consumption significantly if the seal is leaking badly.

During periods of down time when the furnace is kept under negative pressure, air drawn in is also expected to react with the electrode column, especially the hot tip. As the column cools down the rate of these reactions are expected to decrease.

All reactions involving electrode graphite were viewed as unimportant to the ISFP model. For this reason all such reactions were omitted from the model.

5.4.5 Mechanical Effects

Some mechanical effects were discussed in paragraph 3.4.5 (page 33). The reader is referred to this paragraph for details.

a. Slag and metal tapping

The ilmenite-smelting process is operated in a semi-continuous manner. This means that inputs are supplied to the process as continuously as possible, while all products except gas and dust are extracted in batches. This practice results in continuous variation in slag and metal levels in the furnace. The levels of both slag and metal rise as material is fed. The slag level drops when slag is tapped. Both the metal and slag levels drop when metal is tapped.

The varying slag layer thickness and position have a marked influence on the behaviour of the freeze lining. These variations cause the freeze lining's properties to vary in at least two dimensions (radial and axial). The freeze lining was however modelled using a 1-dimensional approach in CHAPTER 3. This was done to simplify the modelling work. This simplification now has a significant impact on how the ISFP model is to be approached. The axial variations caused by varying slag and metal bath levels cannot be described in the ISFP model when using the FLC model to describe the freeze lining. For this reason a simplification had to be introduced (Simplification 5.1, page 113).

It was decided to keep slag and metal bath levels constant in the ISFP model by extracting slag and metal continuously from the system (equivalent to continuous tapping). This is not an accurate description of the actual process, but the consequences of this simplification were accepted within the scope of this study.

b. Cave-in of accretions

Material projected towards the walls by the force of the arc and dust from the freeboard collect on the furnace sidewalls and roof to form accretions. These accretions do not simply grow until the entire freeboard is clogged up, but they are also continuously melted away and dripping into the slag bath. In some cases large pieces of accretions detach from the sidewalls and/or roof and fall into the slag bath. This can cause sudden mixing of portions of the slag and metal baths. Such mixing can cause accelerated reaction between the high carbon metal and the slag.

The cave-in of accretions was not of interest during the current study and this phenomenon was therefore omitted from the ISFP model.

c. Water leaks

Water cooling is used to extract heat from the roof and gas off-take of the furnace. These water cooling systems sometimes rupture or crack, causing water to enter the freeboard or off-gas duct. When the flow of water from such a leak is significant it can result in water reaching the slag bath surface. This poses a very real threat in terms of explosions. Furnaces have been damaged in the past by such explosions.

Water leaks and their influence on the process and equipment were not relevant to this study. These phenomena were therefore omitted from the ISFP model.

5.4.6 Summary of Key Phenomena

The table below summarises the phenomena identified above and assigns a level of importance to each phenomenon within the context of the ISFP model. A level of importance of 1 means that the phenomenon was considered unimportant and it was subsequently ignored. Level 2 indicates that the phenomenon had to be incorporated into the model, but it was not necessary to model it in detail. Level 3 marks critical phenomena that had to be modelled in as much detail as possible.

			Level of importance to current modelling effort		
			1	2	3
Heat transfer	From the arc			✔	
	Between slag bath and metal bath		✔		
	From slag bath surface to freeboard			✔	
	From slag bath to freeze lining and sidewall				✔
	From slag bath to crust and freeboard				✔
	From metal bath to sidewalls and hearth			✔	
	Through upper sidewalls and roof			✔	
Mass transfer	Bulk flow	Feed materials			✔
		Product materials			✔
		Metal droplets through slag bath	✔		
		Gas from slag bath surface into freeboard	✔		
		Gas through slag bath into freeboard	✔		
		Process material to sidewalls and roof	✔		
		Process material from sidewalls and roof into slag bath	✔		
	At slag–reductant interface			✔	
	At interface between slag and metal baths			✔	
	Carbon into metal bath			✔	
	At interface between slag bath and freeze lining			✔	
Momentum transfer	Momentum sources	The arc	✔		
		Feed material	✔		
		Electromagnetic stirring	✔		
		Rising gas	✔		
		Buoyancy forces	✔		
	In the slag bath			✔	
	In the metal bath			✔	
	In the freeboard		✔		
Chemical reaction	Liquid slag	With ilmenite			✔
		With reductant			✔
		With liquid slag			✔
		With liquid metal			✔
		With refractory material	✔		
	Solid slag	With liquid slag			✔
		With solid slag	✔		
		With liquid metal	✔		
	Liquid metal	With reductant		✔	
		With refractory material	✔		
	Reduction product gas	With liquid slag	✔		
		With reductant	✔		
	Air		✔		
	Graphite		✔		
Mechanical effects	Slag and metal tapping		✔		
	Cave–in of accretions		✔		

	Water leaks	✔				

Table 6 – Summary of key phenomena for the ISFP model.

5.5 APPROACH AND MODEL COMPLEXITY

From Table 6 it is clear that heat transfer to the freeze lining and crust, bulk mass flow of feed and product materials, and chemical reactions involving liquid slag are most important to the ISFP model. Details related to the freeze lining and crust have been addressed in the FLC and SBCC models. These models were therefore incorporated into the ISFP model.

Describing bulk flow of mass and energy into and out of the system requires first of all a mass and energy balance. In addition to this some framework is required to model the important reactions taking place at the various phase boundaries. The modelling methodology developed by Pauw (1989) addresses all these requirements and it was therefore chosen as the approach for the ISFP model. Definitions and descriptions of the model elements used in the Pauw approach are given in APPENDIX B.

Within the methodology developed by Pauw (1989) Gibbs-free-energy minimisation is used to model chemical reactions. This was discussed in paragraph 3.5.2 (page 35) and the reader is referred to this paragraph for details.

5.6 MODEL FORMULATION

5.6.1 Assumptions

The following paragraphs list assumptions made as part of the ISFP model formulation. The paragraphs clarify why the assumptions were made, their validity and the impact that the assumptions have on the model.

a. Assumption 5.1

Statement: The slag bath, metal bath and furnace freeboard are all at the same temperature.

Justification: The assumption was made to simplify the model. If the model had to describe different temperatures for the three zones, it would have been significantly more complicated in addition to the fact that other assumptions would have been required to formulate heat transfer between the metal bath and slag bath, and between the slag bath and freeboard.

Validity: The assumption statement is not true in the actual process. It has already been stated that the metal bath is usually colder than the slag bath because the slag bath is located between the metal bath and the arc. A significant amount of heat is also extracted from the metal bath through the lower sidewalls and hearth. Differences between slag and metal temperatures have been reported to be between 50 and 90 °C (Geldenhuis and Pistorius, 1999).

The assumption also does not hold for gas in the freeboard because heat is extracted from this gas by radiation and convection to the furnace roof and walls. It is however

believed that the difference in temperature between freeboard and slag bath will be less than the difference in temperature between the slag and metal baths.

Impact: Inaccuracies were caused by this assumption. The errors made with either slag or metal temperature were expected to be less than the actual difference in temperature between these two phases (between 50 and 90 °C) since the model was configured to calculate an average temperature for the system. Temperature variations in this range proved to have a relatively small effect on the result of equilibrium calculations describing reduction reactions. These calculations were done with FactSage. The inaccuracies associated with the assumption were therefore deemed to be acceptable.

b. Assumption 5.2

Statement: The slag bath is ideally mixed.

Justification: The assumption was introduced to simplify the model. The alternatives to this assumption were the introduction of additional slag mixers in the model, and the development of a complete fluid flow model of the slag bath. Both alternatives introduce significant additional complexity into the model. The first alternative would also required assumptions regarding flow in the bath based on the same information available when the current assumption was made. It did not seem that any significant value could be added to the model in this way.

The second alternative could have proved more fruitful, but at the expense of significant additional complexity and longer model execution times.

Validity: The assumption statement is not absolutely true in the actual process. However, due to significant momentum transferred to the slag bath by entering feed material, the arc, electromagnetic forces, rising gas and buoyancy forces, it is expected that this assumption is a fair approximation of conditions in an actual slag bath.

Impact: Because the assumption is not an absolutely accurate description of conditions in the actual process, it caused inaccuracies in the model. Because of the mixing occurring in the slag bath, these inaccuracies were believed to be negligible.

c. Assumption 5.3

Statement: The metal bath is ideally mixed.

Justification: The same justification supplied for Assumption 5.2 holds for this assumption regarding the metal bath.

Validity: This assumption, similar to Assumption 5.2, was believed to be a good approximation of reality. This is due to significant stirring in the metal bath as a result of momentum transferred form the arc, entering feed material, electromagnetic forces and buoyancy forces.

Impact: It was believed that inaccuracies resulting from this assumption were negligible.

d. Assumption 5.4

Statement: Gas in the freeboard is ideally mixed.

Justification: This assumption was made because the gas phase in the furnace freeboard is not very important within the context of the model.

Validity: This assumption was believed to be a fair approximation of the actual condition in the furnace freeboard. The reason for this was the significant fluid flow caused in the freeboard by the arc.

Impact: The assumption had virtually no impact on the model due to the way in which the gas phase was handled in the model. Any gas formed during reduction was simply removed from the system virtually as soon as it was produced.

e. Assumption 5.5

Statement: Gas produced by any form of reduction reaction in the process immediately escapes into the freeboard and does not come into contact with slag, metal or reductant again.

Justification: This assumption was introduced to simplify the model. Without it interfaces between liquid slag and gas and between reductant and gas would have been required. Inclusion of such interfaces in the model would have required more assumptions and would not have added significantly to the functionality of the model.

Validity: It is well known that gas does not instantly escape into the freeboard once formed. Gas formed at the interface between the slag and metal baths has to rise through the slag bath before it reaches the freeboard. Gas formed at the interface between liquid slag and reductant is also expected to remain attached to the reductant particle for at least a small period of time. The assumption statement is therefore not true.

Impact: It was deemed that the impact of this assumption would have negligible influence on the model's accuracy.

f. Assumption 5.6

Statement: No air enters the furnace during operation.

Justification: This assumption was made so that air entrainment could be ignored in the model. The influence of air on the system was not the focus of the study and inclusion of air entrainment would have caused unnecessary complexities in the model. Such inclusion would have required at least one additional assumption to be made anyway.

Validity: Fluctuations in furnace pressure during operation cause air to be drawn into the furnace from time to time. For this reason the assumption statement is not true.

Impact: Air entrainment causes post combustion and a reduction in reductant efficiency. Since air entrainment is not included in the model, these phenomena could not be described by it.

g. Assumption 5.7

Statement: No air enters the furnace during periods of down time.

Justification: This assumption was made for the same reasons as Assumption 5.6.

Validity: The statement of this assumption is certainly not true since large volumes of air are drawn into the furnace while it is under negative pressure during periods of down time.

Impact: This assumption causes inaccuracies in the description of transient behaviour associated with furnace down time. Such behaviour was however not the focus of this study. For this reason such inaccuracies could be tolerated.

5.6.2 Simplifications

The following paragraphs list simplifications that were made in the model. The justification and impact of the simplifications are also presented.

a. Simplification 5.1

Description: The model was configured in such a way that slag and metal were tapped continuously from the furnace.

Justification: This simplification was required because the FLC model used to describe the freeze lining is a one-dimensional model describing melting and solidification in only the radial dimension. This meant that variations in the axial dimension caused by changing slag and metal levels could not be described with the FLC model.

Impact: This simplification caused a significant difference between the dynamic behaviour of the process as described by the ISFP model and the dynamic behaviour of the actual process. Even though this was the case, it was concluded that the description of process behaviour provided by the ISFP model inclusive of this simplification would be adequate given the objectives of the current work.

b. Simplification 5.2

Description: A collection of stoichiometric condensed phases was used to describe ilmenite instead of a collection of solid solution phases.

Justification: This simplification was required because of the fact that no detailed mineralogical analyses of ilmenite were available for use in this study.

Impact: The simplification caused inaccuracies in describing the enthalpy of ilmenite and other of its thermodynamic properties. These inaccuracies were deemed to be acceptable within the context of the ISFP model.

5.6.3 Material Definitions

The definitions of the liquid slag and solid slag materials used in the ISFP model are in many respects identical to the definitions used for the FLC model. For many of the materials used in the ISFP model, the reader is referred back to the definitions made in the chapter describing the FLC model.

a. Ilmenite

The titanium-bearing material fed into the ilmenite-smelting furnace is named Ilmenite within the context of the ISFP model.

Ilmenite was defined to contain the following phases:

- Rutile stoichiometric condensed phase.
- Hematite stoichiometric condensed phase.

- Ilmenite stoichiometric condensed phase.

i. Rutile Stoichiometric Condensed Phase

Actual constituents: It is known that a rutile solid solution can contain TiO_2, Ti_2O_3, ZrO_2 (Eriksson et al., 1996; FactSage 5.2). However, due to no detailed mineralogical analyses being available, a simple stoichiometric condensed phase was used.

Considered constituents: TiO_2.

Solution model: None.

Thermochemical data: ChemSage format data file from GTT Technologies.

ii. Hematite Stoichiometric Condensed Phase

Actual constituents: Hematite occurs as a solid solution (with $FeTiO_3$) in reality (FactSage 5.2). However, due to no detailed mineralogical analyses being available, a simple stoichiometric condensed phase was used.

Considered constituents: Fe_2O_3.

Solution model: None.

Thermochemical data: ChemSage format data file from GTT Technologies.

iii. Ilmenite Stoichiometric Condensed Phase

Actual constituents: In reality ilmenite is a solid solution containing, for example, Ti_2O_3, $MgTiO_3$, $FeTiO_3$ and $MnTiO_3$ (FactSage 5.2). However, due to no detailed mineralogical analyses being available, a simple stoichiometric condensed phase was used.

Considered constituents: $FeTiO_3$.

Solution model: None.

Thermochemical data: ChemSage format data file from GTT Technologies.

b. Reductant

Anthracite and charred coal are used as reductants in the ilmenite-smelting process. These materials contain ash, volatile matter, moisture and carbon. Reductant is however represented here as pure graphite.

Reductant was defined to contain only a single phase, named Graphite Phase.

i. Graphite Phase

Actual constituents: Numerous organic species are found in the carbonaceous phase of coals and anthracite. Detail regarding most of these species was ignored here.

Considered constituents: For the purpose of the ISFP model, the phase was viewed as being pure carbon.

Solution model: None

Thermochemical data: FactSage 5.2. (Bale et al, 2002)

c. Liquid Slag

Refer to paragraph 3.6.3a on page 39.

d. Liquid Metal

Refer to paragraph 3.6.3b on page 39.

e. Gas

Gas is produced as a product of reduction reactions in the process.

Gas was defined to contain only a single phase, named Gas Phase.

i. Gas Phase

Actual constituents:	It is likely that numerous species exist in the gas phase in the actual process. It is virtually impossible to compile a complete list of constituents here.
Considered constituents:	C, C_2, C_3, C_4, C_5, O, O_2, O_3, CO, C_2O, CO_2, C_3O_2, Ar, Ti, TiO, Fe, FeO, and $Fe(CO)_5$. (Of these constituents only CO and CO_2 occurred in significant amounts.)
Solution model:	Ideal mixture.
Thermochemical data:	ChemSage format data file from GTT Technologies.

f. Solid Slag

Refer to paragraph 3.6.3c on page 40.

g. Magnesia Brick

Refer to paragraph 3.6.3d on page 41.

h. Ramming

Refer to paragraph 3.6.3e on page 41.

i. Steel

Refer to paragraph 3.6.3f on page 41.

5.6.4 Model Structure

This paragraph and its sub-paragraphs show and describe the various elements of the ISFP model's structure. The model structure was built using energy and material modules and flow streams as defined by Pauw (1989).

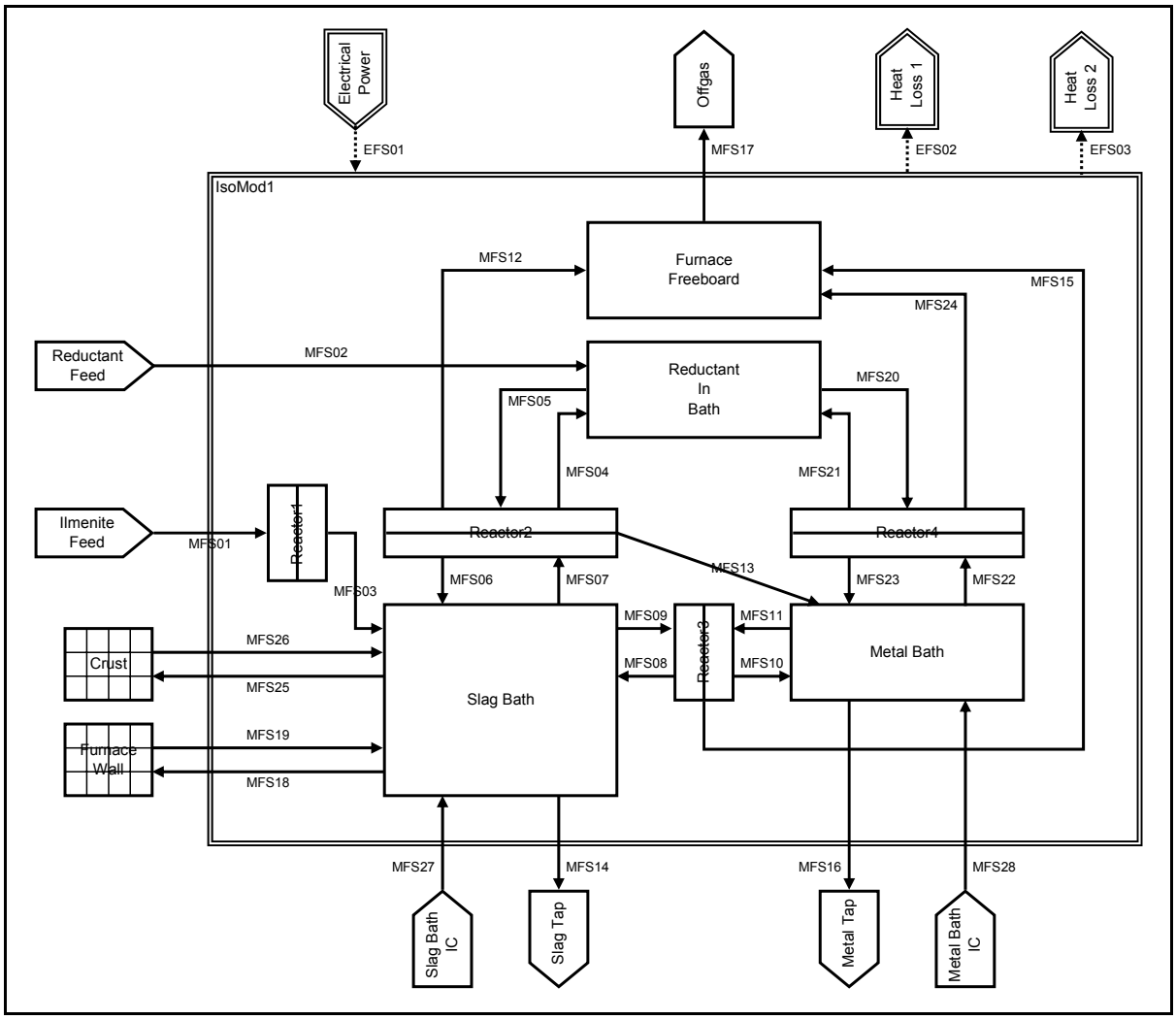

Figure 58 – Flow sheet of ISFP model.

a. Energy Modules

NAME	DESCRIPTION	CALCULATIONS
	Energy Input Modules	
ElectricalPower	This energy input module represents the DC electrical power supply of the furnace. It supplies energy to fuel heating, melting and reduction reactions occurring in the process.	The power supplied via the ElectricalPower module was specified as a fixed parameter forming part of the definition of the scenario being modelled, or as a ratio to the feed rate of the IlmeniteFeed module.
	Energy Output Modules	
HeatLoss1	This energy output module represents a portion of the heat loss from the process that is lost through the upper sidewalls and roof.	None.
HeatLoss2	This energy output module represents heat losses from the process through the lower sidewalls and hearth.	None.
	Isothermal Modules	
IsoMod1	This isothermal module represents virtually the entire content of the furnace. The only exclusions from it are the solid slag of the freeze lining and the solid slag of the crust when a crust is present. Since these parts of the process contain temperature gradients that are important to the current study, they could not be described using an isothermal module.	Enthalpy integration.

Table 7 – Description of energy modules used in the ISFP model.

b. Energy Flow Streams

NAME	DESCRIPTION	CALCULATIONS
EFS01	This energy flow stream delivers energy supplied by the ElectricalPower module to the IsoMod1 module.	None.
EFS02	This energy flow stream calculates the rate at which energy is lost via the upper sidewalls and roof as a result of convection and radiation from the portion of the bath surface that is not covered by the Crust conductor module. It withdraws energy at this rate from the IsoMod1 module and delivers it to the HeatLoss1 module.	§ 5.6.6a, p. 121.
EFS03	This energy flow stream calculates the rate at which energy is lost via the lower sidewalls and hearth that is in contact with the metal bath. It withdraws energy at this rate from the IsoMod1 module and delivers it to the HeatLoss2 module.	§ 5.6.6b, p. 122.

Table 8 – Description of energy flow streams used in the ISFP model.

c. Material Modules

NAME	DESCRIPTION	CALCULATIONS
	Material Input Modules	
SlagBathIC	This material input module does not refer to any physical part of the actual process. It was included into the model to generate an initial condition (IC) of the slag bath state.	The feed rate of the SlagBathIC module was specified as fixed parameters forming part of the definition of the scenario being modelled.
MetalBathIC	This material input module does not refer to any physical part of the actual process. It was included into the model to generate an initial condition (IC) of the metal bath state.	The feed rate of the MetalBathIC module was specified as fixed parameters forming part of the definition of the scenario being modelled.
IlmeniteFeed	This material input module represents the part of the feed system that charges ilmenite into the furnace.	The feed rate of the IlmeniteFeed module was specified as a fixed parameter forming part of the definition of the scenario being modelled.
ReductantFeed	This material input module represents the part of the feed system that charges reductant into the furnace.	The feed rate of the ReductantFeed module was specified as a fixed parameter forming part of the definition of the scenario being modelled, or as a ratio to the feed rate of the IlmeniteFeed module.
	Material Output Modules	
SlagTap	This material output module represents slag being tapped from the furnace through a slag tap hole.	None.
MetalTap	This material output module represents metal being tapped from the furnace through a metal tap hole.	None.
Offgas	This material output module represents gas being extracted from the furnace off-gas system.	None.
	Ideal Mixers	
SlagBath	This mixer represents all liquid slag in the furnace.	Mass integration.
ReductantInBath	This mixer represents all reductant particles in the furnace.	Mass integration.
MetalBath	This mixer represents all liquid metal in the furnace.	Mass integration.
FurnaceFreeboard	This mixer represents all gas in the furnace.	Mass integration.
	Reactors	
Reactor1	This reactor represents the melting of ilmenite occurring in the process as this feed material heats up.	Gibbs-free-energy minimisation.
Reactor2	This reactor represents all reduction reactions taking place at an interface between liquid slag and reductant.	Gibbs-free-energy minimisation.
Reactor3	This reactor represents all reduction reactions taking place at an interface between liquid slag and liquid metal.	Gibbs-free-energy minimisation.
Reactor4	This reactor represents contact between reductant particles and liquid metal in the turbulent zone underneath the electrode. The contact results in dissolution of carbon in liquid metal.	Gibbs-free-energy minimisation.

NAME	DESCRIPTION	CALCULATIONS
	Conductors	
FurnaceWall	This conductor represents the freeze lining and furnace wall.	See CHAPTER 3.
Crust	This conductor represents a solid slag crust that forms on the slag bath surface during periods of down time.	See CHAPTER 4.

Table 9 – Description of material modules used in the ISFP model.

d. Material Flow Streams

NAME	DESCRIPTION	CALCULATIONS
MFS01	This flow stream delivers material supplied by the IlmeniteFeed module to the Reactor1 module.	None.
MFS02	This flow stream delivers material supplied by the ReductantFeed module to the ReductantInBath module.	None.
MFS03	This flow stream delivers ilmenite melted by Reactor1 to the SlagBath module.	None.
MFS04	This flow stream delivers solid carbon not consumed by reduction reactions in Reactor2 to the ReductantInBath module.	None.
MFS05	This flow stream represents reductant involved in reduction reactions due to contact with liquid slag. It draws material from the ReductantInBathModule and delivers it to Reactor2.	§ 5.6.8a, p. 125.
MFS06	This flow stream delivers the liquid slag product of reduction reactions in Reactor2 to the SlagBath module.	None.
MFS07	This flow stream represents liquid slag involved in reduction reactions due to contact with reductant particles. It draws material from the SlagBath and delivers it to Reactor2.	§ 5.6.8a, p. 125.
MFS08	This flow stream delivers the liquid slag product of reduction reactions in Reactor3 to the SlagBath module.	None.
MFS09	This flow stream represents liquid slag involved in reduction reactions due to contact with liquid metal having high carbon content. It draws material from the SlagBath and delivers it to Reactor3.	§ 5.6.8b, p. 129.
MFS10	This flow stream delivers the liquid metal product of reduction reactions in Reactor3 to the MetalBath module.	None.
MFS11	This flow stream represents high-carbon liquid metal involved in reduction reactions due to contact with liquid slag. It draws material from the MetalBath and delivers it to Reactor3.	§ 5.6.8b, p. 129.
MFS12	This flow stream delivers the gaseous product of reduction reactions in Reactor2 to the FurnaceFreeboard module.	None.
MFS13	This flow stream delivers the liquid metal product of reduction reactions in Reactor2 to the MetalBath module.	None.
MFS14	This flow stream represents liquid slag tapped from the furnace through a slag tap hole. It extracts material from the SlagBath module and delivers it to the SlagTap output module.	§ 5.6.7a, p. 124.
MFS15	This flow stream delivers the gaseous product of reduction reactions in Reactor3 to the FurnaceFreeboard module.	None.
MFS16	This flow stream represents liquid metal tapped from the furnace through a metal tap hole. It extracts material from the MetalBath module and delivers it to the MetalTap output module.	§ 5.6.7b, p. 124.
MFS17	This flow stream represents gas extracted from the furnace by the off-gas system. It extracts material from the FurnaceFreeboard module and delivers it to the Offgas module.	None.
MFS18	This flow stream represents liquid slag circulating past the freeze lining due to stirring in the slag bath. It extracts liquid slag from the SlagBath module and delivers it to the FurnaceWall conductor.	§ 5.6.8c.i, p. 131.
MFS19	This flow stream delivers liquid slag that had been melted or that had not been solidified by the FurnaceWall conductor to the SlagBath module.	None.
MFS20	This flow stream represents reductant involved in dissolution reactions due to contact with liquid metal in the turbulent zone underneath the arc. It draws material from the ReductantInBath and delivers it to Reactor4.	§ 5.6.8b.i, p. 129.
MFS21	This flow stream delivers solid carbon not consumed by dissolution in Reactor4 to the ReductantInBath module.	None.
MFS22	This flow stream represents liquid metal involved in dissolution reactions due to contact with reductant particles in the turbulent zone underneath the arc. It draws material from the MetalBath and delivers it to Reactor4.	§ 5.6.8b.i, p. 129.

NAME	DESCRIPTION	CALCULATIONS
MFS23	This flow stream delivers the liquid metal product of dissolution reactions in Reactor4 to the MetalBath module.	None.
MFS24	This flow stream delivers the gaseous product of reactions in Reactor4 to the FurnaceFreeboard module. It is fairly unlikely that gas will be generated by this reactor, but this flow stream was nevertheless added.	None.
MFS25	This flow stream represents liquid slag circulating past the slag bath surface or crust (when it is present) due to stirring in the slag bath. It extracts liquid slag from the SlagBath module and delivers it to the Crust conductor.	§ 5.6.8d.i, p. 132.
MFS26	This flow stream delivers liquid slag that had been melted or that had not been solidified by the Crust conductor to the SlagBath module.	None.
MFS27	This flow stream delivers material supplied by the SlagBathIC module to the SlagBath module.	None.
MFS28	This flow stream delivers material supplied by the MetalBathIC module to the MetalBath module.	None.

Table 10 – Description of material flow streams used in the ISFP model.

5.6.5 From Model Structure to Process Model

The model structure presented above is a representation of the ilmenite-smelting process built by using the language of fairly generic flow streams and modules proposed by Pauw (1989). The flow streams and modules constitute a layer of modelling infrastructure that is able to do the following routine process modelling tasks:

- Mass balancing.
- Energy balancing.
- Temperature calculations.
- Gibbs-free-energy-minimisation calculations.
- One-dimensional conduction combined with solidification and melting.

However useful this layer of infrastructure may seem, it is not yet able to describe the behaviour of the process of interest. Some additional information must be specified and some more knowledge needs to be embedded into the structure before it can be viewed as a complete process model. The following aspects still need to be addressed:

- Specification of initial conditions.
- Specification of model inputs.
- Formulation of sub-models to describe phenomena that influence the dynamic behaviour of the process.
- Specification of values for sub-model parameters.

a. Initial conditions

It is necessary to generate initial conditions for a modelling experiment so that the starting point of the experiment can be controlled. One would not, for example, want to execute an experiment starting with an empty furnace at ambient temperature. It would be far less cumbersome to start the model with filled metal and slag baths with desired compositions, the system at a desired temperature, and some chosen initial states for the freeze lining and crust conductor modules.

In the structure shown in Figure 58 (page 116) all the modules that are able to describe part of the state of the process are candidates for requiring initial conditions. The following is a list of such modules:

- Isothermal modules

  Because isothermal modules contain mixer modules that contain material, an isothermal module itself does not need to be given an initial condition. Proper initialisation of its contained mixers would be adequate.

- Mixers

  The mass and composition of material contained in mixers are initialised by feeding material into these mixers by material input modules that are included into the model structure specifically for the purpose of generating initial conditions. The initial temperature of an isothermal module is set by feeding material into its contained mixers at the desired temperature.

  In the case of the model presented in Figure 58 (page 116) it was decided that only the SlagBath and MetalBath mixers need initial conditions. Material was fed into these mixers at the start of experiments to set up the desired initial conditions.

- Conductor modules

  Conductor models are initialised by specifying an initial steady-state heat flow rate and an initial composition of the solid slag layer if solid slag is present at the specified heat flow rate. In the case of the FurnaceWall conductor this results in an initial temperature profile in each of the conductor layers as well as an initial freeze lining thickness and composition. In the case of the Crust conductor module it results in an initial temperature profile and composition for the solid slag layer if the specified heat flow rate can sustain such a layer.

b. Model inputs

Model inputs refer to parameters in the actual process that are usually manipulated from outside the process. For example, an operator decides on the feed rate at which the process must be operated. Similarly in the case of the model, parameters such as ilmenite feed rate, reductant feed rate, electrical power, and slag and metal tapping rates must be specified as functions of time so that the model can react to the variations in these parameters.

In the case of the ISFP model, however, slag and metal tapping rates were not manipulated as model inputs. Due to Simplification 5.1 (page 113) two very simple sub-models were used to specify the tapping rates. These sub-models are discussed in paragraph 5.6.7 (page 124).

c. Sub-models and their parameters

Initial conditions and specification of model inputs combined with the model structure shown in Figure 58 (page 116) goes some way towards creating a realistic scenario to be used in an experiment. These elements provide a representation of the process, realistic initial conditions of the slag and metal baths in terms of mass, composition and temperature, and even variations in process parameters that can mimic operating conditions that had actually been used on the process or are planned to be used.

One important element is however not yet present; the sub-models that describe the phenomena that determine the dynamic behaviour of the process in question. Without these sub-models, the process model (in the case of the ISFP model) will not function at all. In other cases the model may function, but it may produce entirely unrealistic results.

Sub-models are required for each flow stream (material and energy) of which the flow is not simply the consequence of the behaviour of the module connected at its input end. For example, the flow of MFS01 is simply the consequence of the feed rate, composition and temperature specified as model inputs on the IlmeniteFeed input module. Similarly the flow of MFS12 is defined as a consequence of the results of the Gibbs-free-energy-minimisation calculations done by Reactor2. Finally, the flow definition of MFS19 is the direct consequence of the heat transfer and Gibbs-free-energy-minimisation calculations done by the FurnaceWall conductor module.

In contrast, the flows of MFS05 and MFS07 are not defined because mixers such as the SlagBath and ReductantInBath modules do not by definition push material at a specific flow rate and composition to their output flow streams. In terms of the actual process a sub-model is required for estimating the rate at which liquid slag and reductant are exposed to reduction reactions through contact between these phases. Similarly, sub-models are required for defining the flows of MFS09 and MFS11, MFS20 and MFS22, MFS18, MFS25, MFS14, MFS16, EFS02 and EFS03.

Sub-models involve numerous input and output values in their calculations. These values are classified as follows:

- Input variables
  Input variables change automatically due to calculations performed internally by the ISFP model.
- Output variables
  Output variables are those values calculated by the sub-model as functions of input variables and model parameters.
- Model parameters
  Model parameters are values set by the user of the ISFP model. These parameters are used to fit or tune the ISFP model to describe the actual process more accurately.

The sub-models used for defining the flows of the above-mentioned flow streams are described and formulated in subsequent paragraphs.

5.6.6 Sub-models to Calculate Heat Losses

a. HeatLoss1Rate: Heat losses through upper sidewalls and roof

i. Modelled phenomena

Heat losses from the slag bath surface through the upper sidewalls and roof have been discussed in paragraphs 5.4.1c (page 93) and 5.4.1g (page 93). The reader is referred to these paragraphs for a description of the phenomena described by this sub-model.

ii. Approach

The approach for calculating heat losses from the top of the slag bath that was followed for the SBCC model in CHAPTER 4 was also applied here. The heat lost through the upper sidewalls and roof was therefore based on a simple heat transfer coefficient boundary condition applied at the top of the slag bath. The largest part of this heat loss was already incorporated as a boundary condition in the Crust conductor module. The heat lost from the remaining part of the slag bath surface that was not covered by the Crust conductor module, had to be calculated with this sub-model, and routed to the HeatLoss1 module.

iii. Formulation

The sub-model was formulated with the following equation:

$$Q = h_{effective}.A.\left(T_{slag\ bath\ surface} - T_{environment}\right)$$

SYMBOL	DESCRIPTION	CLASS	UNITS
Q	The rate at which heat is lost through the upper sidewalls and roof as a result of radiation and convection for the part of the slag bath surface not covered by the Crust conductor module.	Output Variable	kW
$h_{effective}$	The effective heat transfer coefficient applied on the slag bath surface to calculate the heat flow rate.	Model Parameter	kW/(m^2.°C)
A	The surface area of the slag bath over which the effective heat transfer coefficient is applied to calculate the heat flow rate.	Model Parameter	m^2
$T_{slag\ bath\ surface}$	The temperature of the slag bath surface. This value is obtained from the uppermost node of the Crust conductor module.	Input Variable	°C
$T_{environment}$	The temperature of the environment outside the furnace (ambient temperature).	Model Parameter	°C

Table 11 – Variables and parameters of the HeatLoss1Rate sub-model of the ISFP model.

iv. Values of model parameters

The value of the surface area model parameter (A) was calculated as the surface area of the bath that was not covered by the Crust conductor module.

Refer to paragraph 4.6.5a (page 73) for details about the effective heat transfer coefficient used here. This model parameter ($h_{effective}$) was set equal to 0.019 kW/(m^2.°C) when the furnace was in operation, and equal to 0.027 kW/(m^2.°C) when the furnace was off.

The value of the ambient temperature model parameter ($T_{environment}$) was set equal to 25 °C.

b. HeatLoss2Rate: Heat losses through lower sidewalls and hearth

i. Modelled phenomena

Heat losses from the metal bath through the lower sidewalls and hearth have been discussed in paragraph 5.4.1f (page 93). The reader is referred to this paragraph for a description of the phenomena described by this sub-model.

ii. Approach

The rate of heat losses through the lower sidewalls and hearth was estimated by a simple calculation. The rate-limiting heat transfer resistance in the heat transfer path was identified and only this resistance was used to calculate the heat flow rate through the wall or hearth.

Heat transfer from the metal bath through both the sidewalls and hearth involves convective heat transfer from the liquid metal to the refractory material surface, conduction through the refractory material, conduction through a ramming layer, conduction through a steel shell, and convection heat transfer from the steel shell to either water or air. In the case of the sidewalls and hearth the largest resistance was calculated to be conduction through the refractory material. This resistance was used to estimate the heat losses. The resistance offered by all other heat transfer steps (convection and conduction through other layers) were ignored. This heat was extracted from the system via the HeatLoss2 energy output module.

iii. Formulation

The sub-model was formulated with the following equation:

$$Q = k_{refractory}\left(T_{average}\right).A_{hearth}.\frac{T_{metal\,bath} - T_{environment}}{\Delta x_{refractory,hearth}} + k_{refractory}\left(T_{average}\right).A_{lower\,sidewall}.\frac{T_{metal\,bath} - T_{environment}}{\Delta x_{refractory,sidewall}}$$

SYMBOL	DESCRIPTION	CLASS	UNITS
Q	The rate at which heat is lost through the lower sidewalls and hearth as a result of convection and conduction.	Output Variable	kW
$k_{refractory}(T)$	The thermal conductivity of the refractory material as a function of temperature. The function for magnesia brick presented in APPENDIX A was used.	Input Variable	kW/(m.°C)
A_{hearth}	The mean surface area over which heat is conducted from the metal bath to the environment through the hearth.	Model Parameter	m^2
$A_{lower\,sidewall}$	The mean surface area over which heat is conducted from the metal bath to the environment through the lower sidewalls.	Model Parameter	m^2
$\Delta x_{refractory,\,hearth}$	The mean distance over which heat is conducted through the hearth.	Model Parameter	m
$\Delta x_{refractory,\,sidewall}$	The mean distance over which heat is conducted through the lower sidewalls.	Model Parameter	m
$T_{metal\,bath}$	The temperature of the metal bath. This value is obtained from the IsoMod1 module containing the MetalBath mixer.	Input Variable	°C
$T_{environment}$	The temperature of the environment outside the furnace (ambient temperature).	Model Parameter	°C
$T_{average}$	The average of $T_{metal\,bath}$ and $T_{environment}$.	Input Variable	°C

Table 12 - Variables and parameters of the HeatLoss2Rate sub-model of the ISFP model.

iv. Values of model parameters

The values of the surface area model parameters (A_{hearth} and $A_{lower\,sidewall}$) and the distance model parameters ($\Delta x_{refractory,\,hearth}$ and $\Delta x_{refractory,\,sidewall}$) were calculated based on the dimensions of the scale drawing shown in Figure 52 (page 90) and paragraph 5.3.1 (page 90).

The value of the ambient temperature model parameter ($T_{environment}$) was set equal to 25 °C.

5.6.7 Sub-models to Calculate Product Flow Rates

a. SlagTapFlow: Tapping rate of slag

i. Modelled phenomena

Slag tapping was discussed in paragraph 5.4.5a (page 108). The way in which it was treated in the ISFP model was different from actual slag tapping due to the introduction of Simplification 5.1 (page 113). The reader is referred to these paragraphs for a description of the phenomena described by this sub-model.

ii. Approach

The introduction of Simplification 5.1 required that the mass of material contained in the SlagBath module remained constant after initial conditions had been established. For this reason the flow rate of slag through the SlagTap module had to be calculated in such a way that a constant slag bath mass was achieved. This was done by simply calculating the difference between the current slag bath mass and the initial slag bath mass. This mass was used to calculate the tapping flow rate.

iii. Formulation

The sub-model was formulated with the following equation:

$$\dot{m}^t = \frac{m^{t-1} - m^0}{\Delta t}$$

SYMBOL	DESCRIPTION	CLASS	UNITS
$\dot{m}^t$	The rate at which slag is tapped from the furnace during time step *t*.	Output Variable	kg/h
m^{t-1}	The mass of slag in the SlagBath module at the end of time step *t-1*.	Input Variable	kg
m^0	The mass of slag with which the SlagBath module was initialised.	Input Variable	kg
Δt	The integration time step of the ISFP model.	Input Variable	h

Table 13 - Variables and parameters of the SlagTapFlow sub-model of the ISFP model.

b. MetalTapFlow: Tapping rate of metal

i. Modelled phenomena

Metal tapping was discussed in paragraph 5.4.5a (page 108). The way in which it was treated in the ISFP model was different from actual metal tapping due to the introduction of Simplification 5.1 (page 113). The reader is referred to these paragraphs for a description of the phenomena described by this sub-model.

ii. Approach

The introduction of Simplification 5.1 required that the mass of material contained in the MetalBath module remained constant after initial conditions had been established. For this reason the flow rate of metal through the MetalTap module had to be calculated in such a way that a constant metal bath mass was achieved. This was done by simply calculating the difference between the current metal bath mass and the initial metal bath mass. This mass was used to calculate the tapping flow rate.

iii. Formulation

The sub-model was formulated with the following equation:

$$\dot{m}^t = \frac{m^{t-1} - m^0}{\Delta t}$$

SYMBOL	DESCRIPTION	CLASS	UNITS
$\dot{m}^t$	The rate at which metal is tapped from the furnace during time step *t*.	Output Variable	kg/h
m^{t-1}	The mass of metal in the MetalBath module at the end of time step *t-1*.	Input Variable	kg
m^0	The mass of metal with which the MetalBath module was initialised.	Input Variable	kg
Δt	The integration time step of the ISFP model.	Input Variable	h

Table 14 - Variables and parameters of the MetalTapFlow sub-model of the ISFP model.

5.6.8 Sub-models to Calculate Mass Transfer Rates to Phase Boundaries

a. Reactor2Flow: Mass flow to the reductant-slag interface

i. Modelled phenomena

Mass transfer to the reductant-slag interface has been discussed in paragraph 5.4.2d (page 96) and chemical reaction between slag and reductant in paragraph 5.4.4a.ii (page 104). The reader is referred to these paragraphs for background on these phenomena.

This sub-model was required calculate the rates at which liquid slag and reductant are exposed to reduction reactions due to contact between these phases. Because contact between solid particles and a liquid plays a large part in this rate, it is useful to track the path of reductant particles from the point of entry into the furnace to the likely points at which these particles are completely consumed.

Reductant particles enter the furnace together with ilmenite particles through the hollow electrode in a mass ratio of around 1:10. The particles fall down the electrode and into the arc, coming in contact with high temperature plasma (12,000 to 18,000 K for plasma without feed (Stenkvist and Bowman, 1987)). Feed material travelling through the plasma cools down the plasma to some degree. The temperatures in the arc are nevertheless expected to be extremely high. The temperature of the cathode spot that should not be influenced strongly by the introduction of feed has been reported to be around 4000 °C (Stenkvist and Bowman, 1987). The sudden rise in temperature around reductant particles is likely to cause thermal shock and initiate devolatalisation, resulting in at least some of these particles breaking up.

The flow patterns in the arc are likely to project some reductant particles toward the furnace walls. The bulk of the particles should however pass through or past the arc in to the turbulent zone underneath the arc. Here the particles come into contact with liquid slag and probably some liquid metal. The flow patterns in this zone likely result in the newly introduced feed material to be carried down and away from the centre of the furnace. The ilmenite particles that have not melted up to this point are likely to do so and then coalesce with the liquid slag phase. Due to the difference in density between reductant (1700 kg/m^3 for

graphite) and liquid slag (3800 kg/m^3), buoyancy forces will tend to push reductant particles to the slag bath surface. These forces may however be opposed by flow patterns in the liquid slag bath.

Depending on the rate of reaction between liquid slag and reductant, small reductant particles may never arrive at the surface of the slag bath but be consumed while submerged. Larger particles may end up at the surface where they will be only partially surrounded by liquid slag. This will result in only part of their surface area being exposed to contact and reaction with liquid slag.

From the above it is obvious that a multitude of complex phenomena combine to determine the total reductant surface area exposed to contact with liquid slag. Detailed modelling of all these phenomena was outside the scope of this study. However, it was still necessary to create some basis, however conjectural, from which the rates of exposure of liquid slag and reductant could be calculated.

Another distinctive phenomenon that had to be addressed by this sub-model was the cause behind the compositional invariance of the slag composition close to the M_3O_5 composition (Figure 59). From experimental results provided in CHAPTER 6 and CHAPTER 7 it seems unlikely that the explanation for the compositional invariance lies in phase chemistry effects as initially suggested by Pistorius (2002). The explanation is therefore likely to be found in some kinetic mechanism. Since detailed knowledge of such a mechanism is not available, one has to rely on data regarding the effects of the mechanism in attempts to mimic its behaviour in the ISFP model. The simplest characterisation of the mechanism's effects is the relationship between equivalent mass $\%Ti_2O_3$ and equivalent mass %FeO reported by Pistorius (2002).

The relationship for the M_3O_5 composition is as follows (dotted line in Figure 59):

$$Equivalent\ \%Ti_2O_3 = -2.0722.Equivalent\ \%FeO + 64.282$$

Based on the results of actual furnaces published by Pistorius (2002) the following relationship was decided on for use in this sub-model (solid line in Figure 59):

$$Equivalent\ \%Ti_2O_3 = -2.0722.Equivalent\ \%FeO + 61.6$$

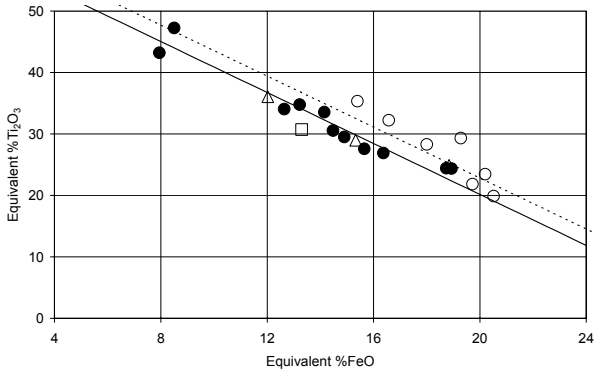

Figure 59 – Compositional invariance of ilmenite smelter slags close to M_3O_5 composition.

The symbols indicate actual industrial data points. The dotted line at the top is the stoichiometric M_3O_5 composition and the solid line is the fitted relationship used in the Reactor2 sub-model (Pistorius 2002).

ii. Approach

The approach used in this sub-model started with calculating an estimated total surface area of all reductant particles in the ReductantInBath mixer. This calculation is based on the assumption that all reductant particles are perfectly spherical. A single surface-area-averaged particle diameter ($D_{average}$) was used to describe the size distribution of the entire population of reductant particles. This diameter was used to calculate the number of particles in the system and the surface area of a single particle. The product of these two results yielded an estimate of the total surface area of all reductant particles in the system.

The surface area then needed to be converted to volume of liquid slag and volume of reductant to be involved in reduction reactions. This was done by assuming a layer thickness for each of these materials (Δr_{slag} and $\Delta r_{reductant}$). For example, it could be assumed that a 1 mm layer of slag around a reductant particle of size $D_{average}$ combined with a 0.2 mm layer of reductant in the particle to participate in reduction reactions during one time step. These layer thicknesses were used to calculated volumes, and the volumes were converted to masses by multiplication with material densities. The masses were converted to mass flow rates by dividing them by the integration time step size of the ISFP model.

The composition of the liquid slag produced by reduction reactions at the reductant-slag interface had to be maintained close to the compositional relationship between Ti_2O_3 and FeO described above. The Gibbs-free-energy-minimisation routine could not be used for this purpose because this would have involved modification of thermochemical data to manipulate the system into displaying the observed kinetic behaviour. It was therefore decided to manipulate the composition of the liquid slag stream flowing to the reductant-slag interface. The purpose of the manipulation was to control the extents to which the following reactions occurred:

$$2TiO_2 + C \rightarrow Ti_2O_3 + CO$$

$$FeO + C \rightarrow Fe + CO$$

When the extents of these reactions are simply allowed to be calculated by the Gibbs-free-energy-minimisation routine (equilibrium) too much Ti_2O_3 is produced. The sub-model therefore had to restrict the extent of the first reaction. The desired results were achieved by controlling the amounts of TiO_2 and Ti_2O_3 allowed to reach the interface.

The approach just described represents a mass transfer restriction applied as part of the Reactor2Flow sub-model. By doing this it is not implied that mass transfer is the cause of the compositional invariance in the actual process. It is simply used as a means to reproduce the effects of whatever mechanism is responsible for the invariance.

iii. Formulation

The sub-model formulation consists of the following equations:

$$n^t_{reductant\ particles} = m^t_{reductant} \div \left[\tfrac{4}{3}\pi \left(\frac{D_{average}}{2} \right)^3 . \rho_{reductant} \right]$$

$$A^t_{total} = 4\pi\left(\frac{D_{average}}{2}\right)^2 .n^{t-1}_{reductant\ particles}$$

$$\dot{m}^t_{liquid\ slag} = n^{t-1}_{reductant\ particles}.\left[\tfrac{4}{3}\pi\left(\frac{D_{average}}{2}+\Delta r_{slag}\right)^3 - \tfrac{4}{3}\pi\left(\frac{D_{average}}{2}\right)^3\right].\rho_{slag} \div \Delta t$$

$$\dot{m}^t_{reductant} = n^{t-1}_{reductant\ particles}.\left[\tfrac{4}{3}\pi\left(\frac{D_{average}}{2}\right)^3 - \tfrac{4}{3}\pi\left(\frac{D_{average}}{2}-\Delta r_{reductant}\right)^3\right].\rho_{reductant} \div \Delta t$$

Because of the simplified liquid slag phase used in the ISFP model, the relationship between equivalent mass $\%Ti_2O_3$ and equivalent mass %FeO could be rewritten as:

$$\%Ti_2O^t_3 = -2.0722.\%FeO^t + 61.6$$

SYMBOL	DESCRIPTION	CLASS	UNITS
A^t_{total}	The total surface area of all reductant particles in the system at the end of time step *t-1*.	Output Variable	m^2
$D_{average}$	The surface-area-averaged diameter of reductant particles in the system.	Model Parameter	m
$\%FeO^t$	The FeO content of the liquid slag at the end of time step *t*.	Input Variable	Mass %
$m^t_{reductant}$	The total mass of reductant in the system at the end of time step *t*.	Input Variable	kg
$\dot{m}^t_{liquid\ slag}$	The mass flow rate of liquid slag to the reductant-slag interface during time step *t*.	Output Variable	kg/h
$\dot{m}^t_{reductant}$	The mass flow rate of reductant to the reductant-slag interface during time step *t*.	Output Variable	kg/h
$n^t_{reductant\ particles}$	The number of reductant particles in the system at the end of time step *t*.	Output Variable	
Δr_{slag}	The layer thickness of slag that is involved in reduction reactions at the reductant-slag interface. The parameter is expressed per unit time to make it independent of the model's integration time step size.	Model Parameter	m/h
$\Delta r_{reductant}$	The layer thickness of reductant that is involved in reduction reactions at the reductant-slag interface. The parameter is expressed per unit time to make it independent of the model's integration time step size.	Model Parameter	m/h
$\rho_{reductant}$	The density of reductant.	Model Parameter	kg/m^3
ρ_{slag}	The density of liquid slag.	Model Parameter	kg/m^3
$\%Ti_2O^t_3$	The Ti_2O_3 content of the liquid slag at the end of time step *t*.	Input Variable	Mass %
Δt	The integration time step of the ISFP model.	Input Variable	h

Table 15 – Variables and parameters of the Reactor2Flow sub-model of the ISFP model.

iv. Values of model parameters

Because reductant particles fed into an ilmenite-smelting furnace are generally smaller than 10 mm diameter, the value of the $D_{average}$ model parameter was varied between 0.1 and 10 mm.

The values of the layer thickness parameters (Δr_{slag} and $\Delta r_{reductant}$) were dependent on the value of $D_{average}$. The layer thicknesses were adjusted in such a way that the mass of liquid slag involved in reduction reactions was always significantly more than the mass of reductant. If this was not done, reduction products were produced that are not observed in the actual process.

Values for the density model parameters were taken from APPENDIX A.

b. Reactor3Flow: Mass flow to the interface between the slag and metal baths

i. Modelled phenomena

Mass transfer to the interface between the slag and metal baths has been discussed in paragraph 5.4.2e (page 97) and chemical reaction between liquid slag and liquid metal in paragraph 5.4.4a.iv (page 105). The reader is referred to these paragraphs for background on these phenomena.

This sub-model was required to calculate the rates at which liquid slag and liquid metal are exposed to reduction reactions due to contact between these phases.

Because it is likely that most of the reduction reactions between these two phases will occur in the vicinity of the interface between the two baths, the surface area of this interface can be used as a basis for calculating flow rates to the phase boundary. It is expected that the actual surface between the slag and metal baths is not flat during operation. The reason for this is stirring in both the metal and slag baths, and the turbulence in the zone underneath the electrode. It is likely that some metal droplets will enter the bulk slag phase near the interface between the two baths, and similarly that some slag droplets will enter the bulk metal phase. Such droplets will off course tend to rejoin their bulk phases due to the difference in density between liquid slag and metal.

Due to the influences of stirring on the interface between the two baths the actual contact surface area between liquid metal and slag will be larger than a flat circular surface between the two baths. The area of such a surface can however provide a good starting point for estimating the surface area of contact.

ii. Approach

The inner diameter of the refractory brick at the axial position of the interface between the slag and metal baths was used as the basis for estimating the surface area between the two phases. Since it is known that the actual surface area is larger than such a flat circular surface, a multiplication factor was used to arrive at a final estimation of the contact surface area. Once this area was available, the approach used in the Reactor2Flow sub-model to estimate the volumes of the two phases to involve in reduction reactions was also applied here.

Two layer thicknesses (Δz_{slag} and Δz_{metal}) were assumed. These layer thicknesses were used to calculate volumes of liquid slag and liquid metal, and the volumes were converted to mass by multiplication with the density of each material.

It was also necessary to apply the same approach as in the Reactor2Flow sub-model for mimicking the compositional invariance of the liquid slag close to the M_3O_5 composition.

iii. Formulation

The sub-model formulation consists of the following equations:

$$A = \alpha.\left(\pi r_{refractory\ inner}^{\ 2}\right)$$

$$\dot{m}^{t}_{liquid\ slag} = \frac{A.\Delta z_{slag}.\rho_{slag}}{\Delta t}$$

$$\dot{m}^{t}_{liquid\ metal} = \frac{A.\Delta z_{metal}.\rho_{metal}}{\Delta t}$$

$$\%Ti_2O_3^t = -2.0722.\%FeO^t + 61.6$$

SYMBOL	DESCRIPTION	CLASS	UNITS
A	The total contact surface area between liquid slag and liquid metal.	Output Variable	m^2
α	The multiplication factor used to estimate the total contact surface area between liquid metal and liquid slag.	Model Parameter	
$\%FeO^t$	The FeO content of the liquid slag at the end of time step *t*.	Input Variable	Mass %
$\dot{m}^{t}_{liquid\ slag}$	The mass flow rate of liquid slag to the slag-metal interface during time step *t*.	Output Variable	kg/h
$\dot{m}^{t}_{liquid\ metal}$	The mass flow rate of liquid metal to the slag-metal interface during time step *t*.	Output Variable	kg/h
$r_{refractory\ inner}$	The inner diameter of the refractory lining at the axial position of the interface between the slag and metal baths.	Model Parameter	m
ρ_{metal}	The density of liquid metal.	Model Parameter	kg/m^3
ρ_{slag}	The density of liquid slag.	Model Parameter	kg/m^3
$\%Ti_2O_3^t$	The Ti_2O_3 content of the liquid slag at the end of time step *t*.	Input Variable	Mass %
Δt	The integration time step of the ISFP model.	Input Variable	h
Δz_{slag}	The layer thickness of slag that is involved in reduction reactions at the slag-metal interface. The parameter is expressed per unit time to make it independent of the model's integration time step size.	Model Parameter	m/h
Δz_{metal}	The layer thickness of metal that is involved in reduction reactions at the slag-metal interface. The parameter is expressed per unit time to make it independent of the model's integration time step size.	Model Parameter	m/h

Table 16 - Variables and parameters of the Reactor3Flow sub-model of the ISFP model.

iv. Values of model parameters

A value for the $r_{refractory\ inner}$ model parameter was obtained from the scale drawing and dimensions presented in Figure 52 (page 90) and paragraph 5.3.1 (page 90).

The values of parameters α, Δz_{slag} and Δz_{metal} were adjusted together with a number of parameters of other sub-models until the ISFP model produced realistic results.

Values for the density model parameters were taken from APPENDIX A.

c. Reactor4Flow: Mass flow to the reductant-metal interface

i. Modelled phenomena

Mass transfer of carbon into the metal bath to the interface between the slag and metal baths has been discussed in paragraph 5.4.2f (page 97). The reader is referred to this paragraph for background on this phenomenon.

ii. Approach

Because very little is known about mechanisms occurring in the turbulent zone underneath the arc where it is believed that reductant particles come into contact with liquid metal, a very simple approach was used in this sub-model. A fraction of the reductant present in the ReductantInBath mixer was simply routed to Reactor4 to come into contact with liquid metal. The same was done with liquid metal from the MetalBath mixer.

iii. Formulation

The sub-model formulation consists of the following equations:

$$\dot{m}^{t}_{reductant} = \frac{\chi_{reductant}.m^{t-1}_{reductant}}{\Delta t}$$

$$\dot{m}^{t}_{liquid\ metal} = \frac{\chi_{liquid\ metal}.m^{t-1}_{liquid\ metal}}{\Delta t}$$

SYMBOL	DESCRIPTION	CLASS	UNITS
$m^{t}_{liquid\ metal}$	The mass of liquid metal present in the MetalBath mixer at the end of time step *t*.	Input Variable	kg
$m^{t}_{reductant}$	The mass of liquid reductant present in the ReductantInBath mixer at the end of time step *t*.	Input Variable	kg
$\dot{m}^{t}_{liquid\ metal}$	The mass flow rate of liquid metal to the reductant-metal interface during time step *t*.	Output Variable	kg/h
$\dot{m}^{t}_{reductant}$	The mass flow rate of reductant to the reductant-metal interface during time step *t*.	Output Variable	kg/h
Δt	The integration time step of the ISFP model.	Input Variable	h
$\chi_{liquid\ metal}$	The fraction of liquid metal routed to the reductant-metal interface.	Model Parameter	
$\chi_{reductant}$	The fraction of reductant routed to the reductant-metal interface.	Model Parameter	

Table 17 - Variables and parameters of the Reactor4Flow sub-model of the ISFP model.

iv. Values of model parameters

The values of the model parameters $\chi_{liquid\ metal}$ and $\chi_{reductant}$ were adjusted to achieve realistic results with the ISFP model.

d. FreezeLiningFlow: Mass flow to interface between liquid slag and freeze lining

i. Modelled phenomena

Due to significant stirring in the slag bath, liquid slag is circulated past the interface between the freeze lining and the liquid slag bath. This contact between the freeze lining and liquid slag causes heat transfer from liquid slag to the freeze lining and ultimately solidification and melting of the freeze lining. The purpose of the FreezeLiningFlow sub-model is to calculate the mass of liquid slag that must flow to the FurnaceWall conductor for participation in heat transfer, and solidification and melting.

ii. Approach

The liquid slag flow to the freeze lining was assigned a lower priority than the flows to tapping, to the reductant-slag interface and to the slag-metal interface. For this reason this sub-model calculates its flow output by simply taking a fraction of the liquid slag left in the SlagBath mixer after the flows of the SlagTapFlow, Reactor2Flow and Reactor3Flow sub-models had been removed from the mixer. This fraction is the model's only parameter and can be used to adjust the ISFP model's overall behaviour.

iii. Formulation

The sub-model was formulated with the following equation:

$$\dot{m}^t = \frac{\chi_{FreezeLiningFlow} \cdot \left(m^{t-1} - \left(\dot{m}^t_{SlagTapFlow} + \dot{m}^t_{Reactor2Flow} + \dot{m}^t_{Reactor3Flow} \right) \Delta t \right)}{\Delta t}$$

SYMBOL	DESCRIPTION	CLASS	UNITS
$\dot{m}^t$	The rate at which slag flows to the interface between liquid slag and the freeze lining during time step *t*.	Output Variable	kg/h
$\chi_{FreezeLiningFlow}$	The fraction of liquid slag to be removed from the SlagBath module and sent to the FurnaceWall conductor.	Model Parameter	
m^{t-1}	The mass of slag in the SlagBath module at the end of time step *t-1*.	Input Variable	kg
$\dot{m}^t_{SlagTapFlow}$	The tapping flow rate of liquid slag during time step *t*.	Input Variable	kg
$\dot{m}^t_{Reactor2Flow}$	The rate at which liquid slag flows to the interface between liquid slag and reductant during time step *t*.	Input Variable	kg
$\dot{m}^t_{Reactor3Flow}$	The rate at which liquid slag flows to the interface between liquid slag and liquid metal during time step *t*.	Input Variable	kg
Δt	The integration time step of the ISFP model.	Input Variable	s

Table 18 - Variables and parameters of the FreezeLiningFlow sub-model of the ISFP model.

iv. Values of model parameters

The value of the model parameter $\chi_{FreezeLiningFlow}$ was set equal to a value between 0 and 1. The sum of this model parameter and its equivalent in the CrustFlow sub-model ($\chi_{CrustFlow}$) had to be greater than or equal to 0 and less than or equal to 1.

e. CrustFlow: Mass flow to interface between liquid slag and crust

i. Modelled phenomena

Due to significant stirring in the slag bath liquid slag is circulated past the interface between the slag bath surface or crust (when it is present) and the liquid slag bath. This contact between the crust and liquid slag causes heat to be transferred from liquid slag to the crust, and ultimately solidification and melting of the crust. The purpose of the CrustFlow sub-model is to calculate the mass of liquid slag that must flow to the Crust conductor for participation in heat transfer, and solidification and melting.

ii. Approach

The approach used for this sub-model was exactly the same as for the FreezeLiningFlow sub-model. Please refer to paragraph 5.6.8d.ii on page 132.

iii. Formulation

The sub-model was formulated with the following equation:

$$\dot{m}^t = \frac{\chi_{CrustFlow} \cdot \left(m^{t-1} - \left(\dot{m}^t_{SlagTapFlow} + \dot{m}^t_{Reactor2Flow} + \dot{m}^t_{Reactor3Flow} \right) \Delta t \right)}{\Delta t}$$

SYMBOL	DESCRIPTION	CLASS	UNITS
$\dot{m}^t$	The rate at which slag flows to the interface between liquid slag and the crust during time step *t*.	Output Variable	kg/h
$\chi_{CrustFlow}$	The fraction of liquid slag to be removed from the SlagBath module and sent to the Crust conductor.	Model Parameter	
m^{t-1}	The mass of slag in the SlagBath module at the end of time step *t-1*.	Input Variable	kg
$\dot{m}^t_{SlagTapFlow}$	The tapping flow rate of liquid slag during time step *t*.	Input Variable	kg
$\dot{m}^t_{Reactor2Flow}$	The rate at which liquid slag flows to the interface between liquid slag and reductant during time step *t*.	Input Variable	kg
$\dot{m}^t_{Reactor3Flow}$	The rate at which liquid slag flows to the interface between liquid slag and liquid metal during time step *t*.	Input Variable	kg
Δt	The integration time step of the ISFP model.	Input Variable	s

Table 19 - Variables and parameters of the CrustFlow sub-model of the ISFP model.

iv. Values of model parameters

The value of the model parameter $\chi_{CrustFlow}$ was set equal to a value between 0 and 1. The sum of this model parameter and its equivalent in the FreezeLiningFlow sub-model ($\chi_{FreezeLiningFlow}$) had to be greater than or equal to 0 and less than or equal to 1.

5.7 MODEL SOLUTION

Solution of the ISFP involved the following steps:

- Assign initial conditions to all modules that contain state.
- Solve the set of differential equations at each time step using Euler integration.

The size of the integration time step was set at 30 seconds.

5.7.1 Initial Conditions

The ISFP model has six modules that contain state and therefore require initial conditions. The modules include the following:

- FurnaceWall conductor module
  The initial conditions of this module were discussed in paragraph 3.7.2 (page 50).
- Crust conductor module
  The initial conditions of this module were discussed in paragraph 4.7.2 (page 78)
- SlagBath ideal mixer module
  The SlagBathIC material input module was used to add an initial mass of liquid slag to the furnace. The added mass filled the empty space between the slag and metal bath surfaces that had not already been filled with solid slag from the freeze lining (see Figure 52 on page90).
- MetalBath ideal mixer module
  The MetalBathIC material input module was used to add an initial mass of liquid metal to the furnace. The added mass filled the volume below the metal bath surface (see Figure 52 on page90).
- ReductantInBath ideal mixer module
  This mixer was left empty.
- FurnaceFreeboard ideal mixer module
  This mixer was left empty.

5.7.2 Solution

The model flow sheet shown in Figure 58 (page 116) represents a set of differential equations that needs to be integrated with respect to time. The integration was done at time steps of 30 seconds using the Euler method. At each time step all of the data associated with each module and flow stream was logged to a database. Model results were drawn from this database.

5.8 MODEL VALIDATION

5.8.1 Purpose

The purpose of validation is to verify the numerical integrity of the ISFP model (Thomas and Brimacombe, 1997).

5.8.2 Objectives

Model validation had to achieve the following objectives:

- Confirm that the basic mass and energy balancing of the model is functioning properly.
- Confirm that the FurnaceWall conductor (FLC model) produced realistic results within the ISFP model.
- Confirm that the Crust conductor (SBCC model) produced realist results within the ISFP model.
- Confirm that Reactor1 is able to heat and melt incoming ilmenite and produce realistic results.
- Confirm that Reactor2 is able to reduce slag with reductant and produce realistic results.

- Confirm that Reactor3 is able to reduce slag with carbon dissolved in liquid metal and produce realistic results.
- Confirm that Reactor4 is able to dissolve carbon into liquid metal realistic results.

5.8.3 Methodology

Because of the complexity of the ISFP model compared with the FLC and SBCC models, it was not possible to create an analytical solution as a reference during model validation. For this reason the most basic check of mass and energy balancing was the starting point of validation. The inputs, outputs and internal quantities of the model were compared and evaluated using mass and energy balances.

The next step was to run the model and, based on experience with actual ilmenite-smelting furnaces, determine whether the various modules in the model produced realistic results. This involved detailed inspection of data generated by the model. For example, the input flow stream compositions and temperatures of Reactor2 were compared with that of the output flow streams and with the enthalpy change calculated by the Gibbs-free-energy-minimisation routine under various circumstances. The functioning of the other reactors and conductor modules was studied in a similar way.

While studying results of the various modules, adjustments were made to the sub-models to produce more realistic results. This was an iterative and time-consuming process.

5.8.4 Validation Experiments

Numerous experiments were done while validating the model and improving sub-models to enhance the realism of the model's results. Because of the nature of the process followed while doing this, no structured set of validation experiments can be presented here.

5.8.5 Validation Results

The result of the validation phase of the ISFP model was a configuration of modules and sub-models that produced fairly realistic results. Results of specific validation experiments are not presented here, because experimental results provided in CHAPTER 8 and CHAPTER 9 demonstrate most of what was observed during the validation phase. Specifically, mass and energy balance checks are presented with each set of experimental results.

The values of model parameters resulting from the validation exercise are summarized in Table 20.

PARAMETER	VALUE	COMMENTS
	HeatLoss1Rate	
A	5.438 m^2	
$h_{effective}$	0.019 kW/(m2.°C)	When furnace is operational.
	0.027 kW/(m2.°C)	When furnace is off.
$T_{environment}$	25 °C	
	HeatLoss2Rate	
A_{hearth}	61.514 m^2	
$A_{sidewall}$	14.687 m^2	
$\Delta x_{refractory,hearth}$	2.000 m	
$\Delta x_{refractory,sidewall}$	0.500 m	
$T_{environment}$	25 °C	
	SlagTapFlow	
None.		

PARAMETER	VALUE	COMMENTS
	MetalTapFlow	
None.		
	Reactor2Flow	
$D_{average}$	0.005 m	
Δr_{slag}	0.080 m/h	
$\Delta r_{reductant}$	0.0002 m/h	
ρ_{slag}	3800 kg/m^3	
$\rho_{reductant}$	1700 kg/m^3	
	Reactor3Flow	
$r_{refractory\ inner}$	4.425 m	
α	1.0	
Δz_{slag}	0.024 m/h	
Δz_{metal}	0.024 m/h	
ρ_{slag}	3800 kg/m^3	
$\rho_{reductant}$	1700 kg/m^3	
	Reactor4Flow	
$\chi_{liquid\ metal}$	0.049	Fraction per hour
$\chi_{reductant}$	6.000	Fraction per hour
	FreezeLiningFlow	
$\chi_{FreezeLiningFlow}$	0.09	
	CrustFlow	
$\chi_{CrustFlow}$	0.91	

Table 20 - Values of parameters of sub-models of the ISFP model.

5.9 COMPARISON WITH ACTUAL DATA

Due to the confidentiality of most information pertaining to the industrial process, no comparison with actual data could be published here. The author was only able to rely on his own experience with actual industrial ilmenite-smelting processes to do validation of the ISFP model.